Drew University

College of Liberal Arts

Directed evolution of Human Topoisomerase IIα mutants in assessing resistance against chemotherapeutic agents

A Thesis in Biochemistry and Molecular Biology

by

Devan Sutaria

Submitted in Partial Fulfillment

of the Requirements for the Degree of

Bachelors in Science

With Specialized Honors in Biochemistry and Molecular Biology

April 2026

Abstract

Topoisomerase IIα (TopoIIα) is an essential enzyme that regulates DNA topology during replication and chromosome segregation and is a therapeutic target in rapidly proliferating cancers. Chemotherapeutic agents such as Etoposide exploit this activity; however, the emergence of resistance-associated mutations within Topoisomerase IIα complicates treatment selection and limits clinical efficacy.

The objective of this study was to identify amino acid substitutions in human Topo-IIαα that reduce sensitivity to topoisomerase II inhibitors and to evaluate their implications for therapeutic response. The human HTOP2A gene which encodes Human Topoisomerase IIα was subjected to random mutagenesis and expressed in a yeast model system, followed by selection under increasing concentrations of Etoposide to isolate resistant variants. Resistant clones were characterized through sequencing and quantitative survivorship analyses to define resistance phenotypes.

Multiple mutations associated with decreased sensitivity to Etoposide were identified, demonstrating that single amino acid substitutions can significantly impair drug efficacy. The 14 most potent mutations were selected for further examination, revealing clusters in the 448-492 base pair region and near the catalytic Tyr805. The discovered variant R487I possessed the highest resistance of all mutations, displaying greater than 50% resistance even at high concentrations of Etoposide.

These findings provide mechanistic insight into topoisomerase II inhibitor resistance and support the utility of directed evolution approaches in predicting therapeutic response. Furthermore, integrating resistance profiles with survivorship outcomes offers a framework for

evaluating the relative effectiveness of Etoposide in comparison to other topoisomerase-targeting agents and informing more personalized, cost-effective treatment strategies.

Table of Contents

Introduction

Cancer

Cancer, the second leading cause of death both globally and in the United States, is characterized by unregulated cell division as a result of genetic mutations, leading to the proliferation of tumorous cancer cells (Siegel et al. 2024; Patel & Adrada 2024; Elshafei et al. 2023). These tumor cells proceed to proliferate to such an extreme degree, sometimes even outnumbering the healthy cells, that the subject is no longer able to maintain regularity within its internal conditions, referred to as the loss of homeostatic balance, leading to the shutdown of organs and organ systems. Further, if left untreated, these groups of tumorous cells can migrate throughout the host via the body's vessels or ducts, thus allowing for the spread, or metastasis, of the cancer. Trailing only heart disease as the most common cause of death, cancer and its subsequent complications claim 9.7 million lives worldwide per year as of 2024 (*World Health Organization* 2024; *National Cancer Institute* 2025; *American Cancer Society* 2020) -- a tally that has grown with each passing decade.

Current Efforts

Consequently, the century-long movement for a cure to the world's second-deadliest disease spans virtually every developed nation in the world, with funding for advancements in cancer research coming from 107 nations (Schmutz et al. 2019; McIntosh et al. 2023). The United States is the world's largest contributor to cancer research funding, representing over half of the world's funding towards finding a cure (Figure 1). The difficulties in discovering a widespread cure for cancer are extensive and multifaceted, but they universally stem from the primary idea that cancer cells are difficult to distinguish from our own healthy cells. The slight, yet impactful, genetic mutations allow cancer cells to override the cell's normal DNA repair

mechanisms, requiring an external treatment in the form of chemotherapy drugs, radiation, or surgery to ameliorate this issue. However, each of these three classes of common treatment options involves the destruction of not only the cancerous cells, but the body's own healthy cells as well. The major limitation of these treatments is their lack of selectivity, resulting in a significantly reduced healthy cell count, leading to many physiological detriments such as weakened immune system, fatigue, and hair/skin loss (*American Cancer Society* 2020; *National Cancer Institute* 2019*)*.

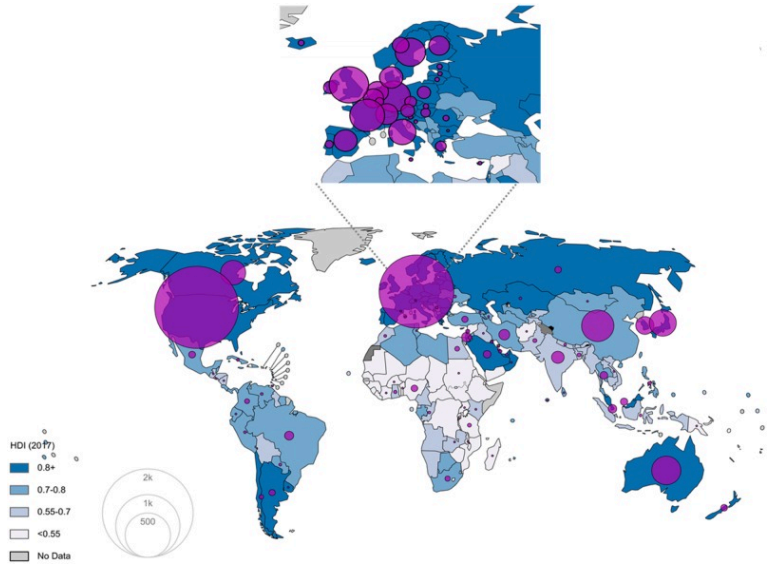

Figure 1 Geographical representation of funding distribution for cancer research efforts. HDI stands for Human Development Index. Darker shades of blue represent higher HDI scores, while lighter shades represent lower scores. Adapted from Schmutz et al. 2019.

DNA

Deoxyribonucleic acid, or DNA, is defined by the National Human Genome Research Institute as "the molecule that carries genetic information for the development and functioning of an organism" (Bates 2026). Through a series of unique nucleotide sequences, the average human

cell contains approximately 3 billion base pairs (National Research Council Committee on Mapping and Sequencing the Human Genome 2016), providing the foundation for messenger ribonucleic acid, or mRNA, production and subsequent protein synthesis. These proteins govern essential cellular functions and maintain physiological stability. Even small alterations in DNA sequence, such as single-nucleotide substitutions, can significantly impact protein structure and function. These mutations, which could arise from errors with the cell's DNA replication machinery, exposure to UV radiation, or several other possibilities (Acuna-Hidalgo et al. 2016; Pfeifer 2020), can disrupt normal gene function and lead to the development of genetic disorders. In cases where mutations alter the structure or expression of critical proteins, conditions such as sickle cell disease, cystic fibrosis, and Down syndrome may arise, reflecting the profound impact that even small changes in DNA sequence can have on organismal health.

Genetic Mutations in Cancer

The potency of cancer revolves around the impact of genetic mutations to make physiological changes in the proteins on which our cells' wellbeing relies (Lichtenstein 2010; Allinen et al. 2004). Referred to as the central dogma of molecular biology, the integrity and composition of a cell's DNA directly influences the final result of the protein for which it codes through a series of transcription and translation. The mutations within cancerous cells disrupt the ideal nucleotide sequence, leading to shortcomings in the protein's function or production as a whole.

The accumulation of genetic mutations extends beyond isolated changes and instead reflects a progressive breakdown of genomic integrity. These mutations can occur in key classes of genes, including proto-oncogenes (normal, healthy genes that regulate cell growth, division, and survival), tumor suppressor genes (genes that work to suppress proliferation of cells), and

genes involved in DNA repair, each contributing to tumor development through distinct mechanisms if their integrity is compromised via spontaneous mutations (*American Cancer Society* 2022). For example, upregulating mutations in proto-oncogenes can drive uncontrolled cell proliferation, while loss-of-function mutations in tumor suppressor genes remove critical regulatory checkpoints that normally restrain cell division. Additionally, defects in DNA repair pathways further accelerate mutation accumulation, creating a cycle of increasing genomic instability. This dynamic mutational landscape not only fuels cancer progression but also generates heterogeneity within tumor cell populations, allowing for the emergence of subclones with selective advantages, including resistance to therapeutic interventions.

Proteins are composed of 20 standard amino acids, which can be broadly categorized based on their chemical properties into 10 nonpolar, five polar uncharged, two negatively charged, and three positively charged residues. A composite list of all 20 amino acids and their respective polarity classifications is included in the Appendix D. Mutations within coding regions are often described using a standardized nomenclature in which the original amino acid, its position, and the substituted amino acid are indicated; for example, G448R denotes a substitution of glycine with arginine at position 448. The functional consequences of such mutations depend on both the properties of the substituted residues and their location within the protein. Some mutations are effectively neutral, either because they do not alter the encoded amino acid due to redundancy in the genetic code or because they occur in non-coding regions of the genome that do not directly influence protein sequence.

Human Topoisomerase IIα

Human Topoisomerase IIα (htopoIIα) is a homodimeric enzyme tasked with facilitating the key processes of DNA replication and transcription through various mechanisms (Barrera et al. 2001; Wendorff et al. 2013; Chen et al. 2016). The enzyme is a dimeric protein with a heart-shaped hole in its center, and works to facilitate its processes through two primary mechanisms (Nielsen et al. 2020): preventing the supercoiling of DNA via inducing double stranded breaks, and assisting in the "unwinding" process that allows each strand of the double helix to serve as a template for a daughter strand, confirming the semiconservative model of DNA replication (Warburton and Earnshaw 1997). The enzyme takes on a similar "untangling" role in cell division to ensure the sister chromatids do not intertwine, or catenate together in a process visualized in Figure 2.

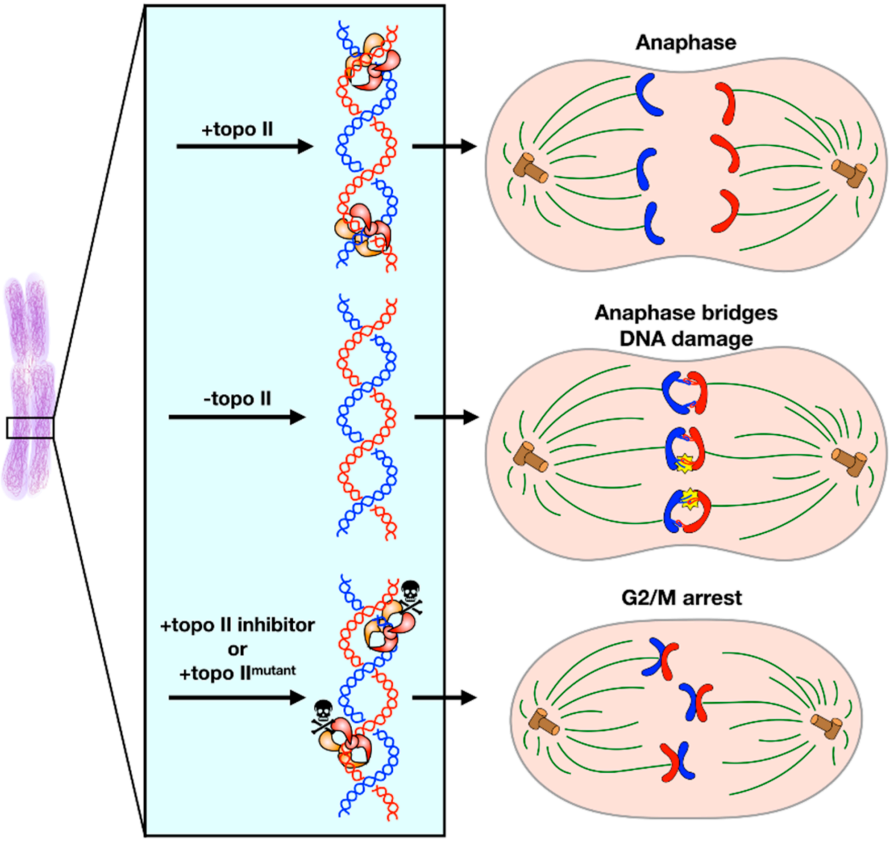

Figure 2 The essential nature of topoisomerase IIα in facilitating proper chromosomal separation during anaphase. Topoisomerase IIα acts as a molecular untangler during cell division (adapted from Lee and Berger 2019).

These temporary double stranded cleavages, as well as the DNA's ability to unwind and "relax," work together to ensure the successful replication or transcription of the double helix. Topoisomerase IIα is essential for a cell's mitotic capabilities, as Human Topoisomerase IIα fosters chromosome condensation and segregation during mitosis (Nielsen 2020). The loss of topoisomerase IIα function, or its temporary inhibition, leads to programmed cell death or mitotic arrest. In contrast, Topoisomerase II-beta is primarily tasked with overseeing and stabilizing the transcriptional progress of transforming DNA codons into their corresponding mRNA product (Mak et al. 2005). mRNA is a single-stranded molecule that serves as the blueprint for protein synthesis. Using DNA as a template to create a near-exact single-stranded copy of each DNA strand, mRNA, and is a powerful tool for treating genetic disorders, such as cancer (Winstead 2022). Though Topoisomerase II-beta is still important for long-term cell viability, it is not considered essential as Topoisomerase IIα (Nielsen 2020).

Topoisomerase IIα's function is tightly coordinated with its distinct structural domains, each contributing to a specific step in the enzyme's catalytic cycle. The N-terminal ATPase domain is responsible for binding and hydrolyzing ATP, a process that drives the large conformational changes necessary for strand passage (Vanden Broeck et al. 2021). Upon ATP binding, the enzyme dimerizes at the ATPase domain, initiating the capture of a DNA segment (the "transported" or T-segment). The central DNA-binding and cleavage domain, often referred to as the catalytic core, mediates the transient double-stranded break in the "gate" (G) segment of DNA, allowing the T-segment to pass through. This cleavage is stabilized by a conserved

tyrosine residue in each subunit, which forms a covalent bond with the DNA backbone (Lindsey Jr. et al. 2014). Following strand passage, ATP hydrolysis triggers enzyme resetting and religation of the G-segment, restoring DNA integrity (Nitiss 2009). The C-terminal domain, while less conserved, is thought to play a role in nuclear localization and interaction with other cellular factors. Altogether, the precise coordination between these structural regions ensures the enzyme's ability to manage DNA topology with high efficiency.

Etoposide Background

In the landscape of chemotherapeutic strategies, one of the hallmark discoveries of the 1960s was the rise in a class of drugs referred to as “topo II inhibitors,” designed to inhibit the action of Topoisomerase IIα (Swedan et al. 2023; Hande 1998). Involved in mitotic capabilities of cell division and DNA replication, Topoisomerase IIα is a valuable target of action for cancer research teams in their search to find a method to halt the unregulated division of certain cells (Cuya et al. 2017). Through a targeted approach, scientists aimed to design drugs that were effective in limiting topoisomerase’s capabilities of inducing double stranded breaks to prevent supercoiling and induce relaxation of the double helix during its replication, leaving the process more prone to errors and more likely to be unsuccessful in creating a copy of the tumor cell DNA.

Due to their target of topoisomerase -- an enzyme present in every nucleated, mitotic cell -- topo II inhibitors are effective against a wide variety of different cancers. Etoposide, in particular, is a common treatment for a wide assortment of cancers. According to the National Library of Medicine, “Etoposide is one of the most widely used cytotoxic drugs and has strong antitumour activity in cases of small-cell lung cancer, testicular cancer, lymphomas and a variety

of childhood malignancies. [Etoposide] is one of the most active single agents in the treatment of small-cell lung cancer (Johnson et al. 1991)"

The intertwined nature of topoisomerase's structure and function offer several specific potential locations of inhibition for cancer drug development teams. Etoposide, one of the most commonly prescribed topoisomerase IIα inhibitors today, works by turning the enzyme's own method against itself. As shown in Figure 3, Etoposide stabilizes the cleavage complex of topoisomerase, effectively freezing the enzyme in a state where DNA remains broken and unable to initiate its repair processes of either homologous repair or non-homologous end joining (Montecucco et. al 2025). This permanent cleavage leads to prolonged DNA damage and, consequently, the death of its host cell. Other topoisomerase II inhibitors can target the ATPase domain to prevent the conformational changes required for strand passage, or the catalytic core to block DNA cleavage and religation. By understanding which domains are responsible for each step in the catalytic cycle, researchers can design drugs with greater specificity and reduced off-target effects.

Etoposide is most commonly administered in combination with a platinum agent, referred to as "EP therapy" (*Macmillan Cancer Support* 2025). Typical Etoposide treatments involve dosages between 15 and 25 μg/mL, offering us a basis for our study. Prescribed in a cycle of 21 to 28 days, the combination treatment is a first-line treatment for a variety of malignancies, most notably ovarian cancers, neuroblastomas, testicular cancer, and small cell lung cancer. Overall, EP chemotherapy ranks as one of the more reliable treatments, especially for rapidly-metastasizing tumors within epithelial tissues. One longitudinal study observing Peripheral T-Cell Lymphoma found that Etoposide treatment increased 5-year overall survival from 39% to 49% (Brink et al. 2022). Further, an EP chemotherapy analysis in 16 Advanced

Thymic Neuroendocrine Neoplasm patients observed an 81.3% disease control rate with median progression-free survival, indicating that the combined treatment modality was extremely effective in improving patient outcomes, extending lifespans by an average of 7.2 months (Guan et al. 2023). With promising anti-tumor capabilities and tangible real-world improvements in progression-free survival, disease control, and overall survival, treatment teams continue to turn to trusted EP paired treatments in the face of rapid-progressing malignancies.

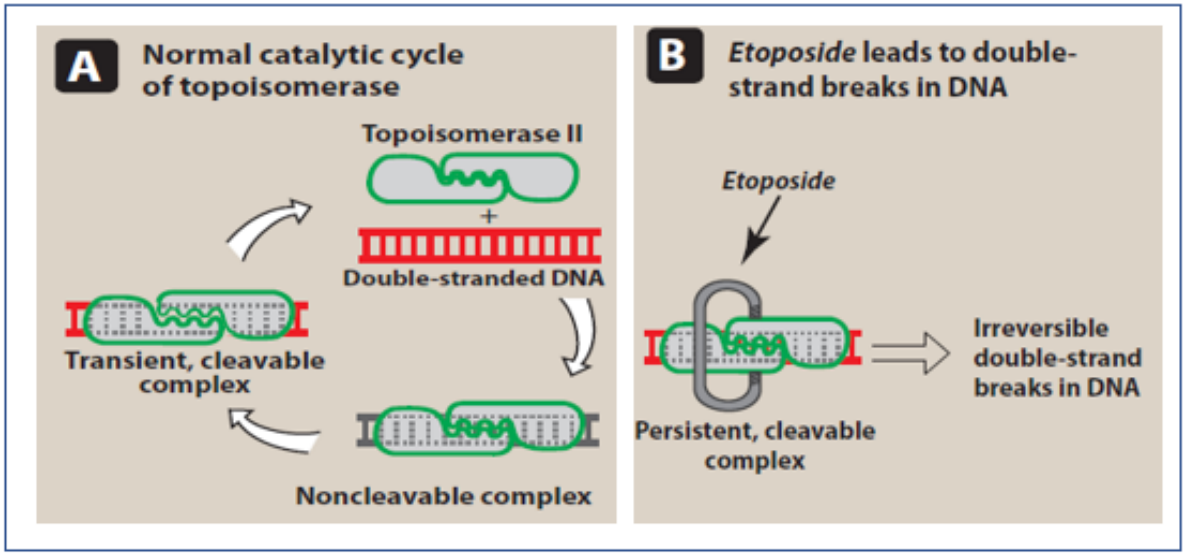

Figure 3 Mechanism of Etoposide action on topoisomerase IIα. Etoposide stabilizes the transient cleavage complex formed between topoisomerase IIα and DNA, preventing religation of double-strand breaks. This results in the accumulation of DNA damage, ultimately leading to cell death (adapted from Whalen et al. 2019).

The structure of Etoposide (Figure 4) is tightly correlated with its function. Etoposide is a semi-synthetic derivative of a plant compound originally isolated from the poisonous mayapple (*Podophyllum peltatum*] (Rima 2020). Its structure is highlighted by a polycyclic ring system, referred to as its Podophyllotoxin core, allowing it to fit into the cleavage gate of topoisomerase

IIα. Podophyllotoxin is the active ingredient in other anti-cancer medications as well given its ability to disrupt microtubule formation; its involvement as the core structural element in Etoposide allows this activity to shift from microtubules to topoisomerase IIα (*National Center for Biotechnology Information* 2024). Etoposide also has both a phenolic hydroxyl group as well as a glycosidic moiety, or sugar group, allowing it to form strong, nearly unbreakable hydrogen bonds with the topoisomerase IIα residues. This sugar group also provides Etoposide with hydrophilic character, allowing for adequate movement throughout the bloodstream and increased cellular uptake. As a potent anti-cancer agent, Etoposide has become a cornerstone therapy for a wide range of human cancers.

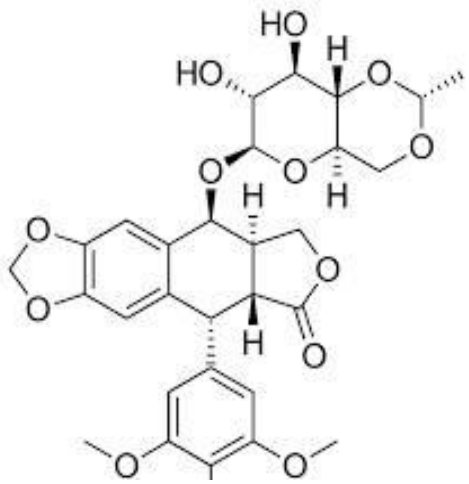

Figure 4: Structure of Etoposide. Etoposide has a polycyclic core, part of the podophyllotoxin family that consists of a variety of anti-cancer medications (adapted from *BioPharma Notes* 2020).

General Drug Resistance

The *National Cancer Institute* defines chemotherapeutic drug resistance as when cancer cells "don't respond to a drug that is usually able to kill or weaken them" (*National Cancer*

Institute 2026*)*. Drug resistance is a multi-faceted hindrance that has plagued drug efficacy across all specialties since their inception. Research and development teams often face difficulties in ensuring their products have proficient longevity, deeming them safe from the body's own resistance mechanisms. The primary difficulty, particularly in designing chemotherapeutic drugs, lies in breadth: cells have evolved several unique mechanisms to undermine the efficacy of drugs (Mollaei et al. 2021). These include alterations to drug targets, increased efflux or decreased uptake of therapeutic agents, enhanced DNA damage repair pathways, and adaptive changes in gene expression that collectively diminish drug potency. In cancer, this problem is exacerbated by pronounced genetic instability, which promotes rapid diversification and enables the selective expansion of resistant subpopulations under therapeutic pressure. Consequently, even highly effective agents may lose clinical utility over time, underscoring the importance of defining resistance mechanisms at the molecular level to guide drug design and strategies to overcome therapeutic failure.

Of the previously mentioned mechanisms, one of the most well-characterized strategies for drug resistance is the overexpression of ATP-binding cassettes, or ABC transporters. These proteins function as efflux pumps that actively export the contents of chemotherapeutic agents out of the cell, reducing the intracellular drug concentration to a greatly-diminished level (Dean 2002). Oftentimes, the resulting level ends up being sub-lethal, thereby saving the cell from the cytotoxic effects of the administered drug. In addition to drug efflux, cancer cells may acquire resistance through dysregulation of apoptotic pathways, often derived from the overexpression of ABC transporters. Under normal conditions, chemotherapeutic-induced DNA damage triggers programmed cell death; however, mutations or altered expression of key apoptotic regulators can allow cancer cells to evade this fate and continue proliferating despite substantial genomic insult.

Furthermore, enhanced DNA repair capacity represents another critical resistance mechanism. Pathways such as non-homologous end joining (NHEJ) and homologous recombination (HR) can become upregulated or more efficient in cancer cells, enabling rapid resolution of drug-induced DNA damage. Collectively, these mechanisms act together to reduce drug sensitivity, allowing tumor cells to survive and expand even in the presence of sustained therapeutic pressure.

In contrast to these broad cellular adaptations, target-based resistance arises from genetic alterations within the target of a chemotherapeutic drug itself is the focus of our study. In the case of topoisomerase II inhibitors such as Etoposide, mutations within the coding sequence of the TOP2A gene can directly modify the structure and function of the Topoisomerase IIα enzyme, leading to disrupted drug binding affinity or catalytic activity. Target-based resistance provides a direct link between genotype and therapeutic response, underscoring the importance of understanding the genetic landscape of the gene encoding for Topoisomerase IIα, referred to as *TOP2A*. Through our study, we aim to be able to predict and overcome resistance to the topoisomerase IIα targeting agent Etoposide.

Etoposide Resistance

Understanding Etoposide's structural basis for activity provides context for how mutations in Topo IIα disrupt drug binding. In the case of topoisomerase IIα, single nucleotide polymorphisms (SNPs), or individual nucleotide alterations as a result of genetic mutations, in the coding region of the Topoisomerase IIα gene have led to resistance against certain inhibitors, rendering individuals possessing these mutations resistant to one of the more effective lines of treatment modalities in the modern drug landscape facing cancer (Jaffrézou et al. 1994). These

mutations have presented a challenge to physicians and scientists alike, as it offers a new variable that can disrupt the efficacy of a drug. Further, this particular variable is undetectable via physical exam or traditional diagnostics like bloodwork, but instead requires genetic testing from biopsy of the cancerous tissue in order to determine whether the patient possesses a mutant form of Human Topoisomerase IIα that renders them resistant to Etoposide. While germline DNA is largely consistent across somatic tissue, cancerous tumor cells arise from somatic cells that acquire oncogenic and tumor-suppressor mutations (Xu et al. 2020). As a result, genetic testing would require analysis of the tumor itself, typically obtained through biopsy. Despite recognition of these resistance-associated mutations, the genetic determinants of Etoposide response remain incompletely characterized, and their mechanistic consequences are not fully understood.

To validate the claim that resistance to Etoposide is based on genetic predisposition, rather than exposure to the drug, Jaffrézou and his colleagues (1994) performed a fluctuation analysis using a clonal cancer cell line. Three groups of ten flasks were seeded with identical populations of more than 2,000 cells each and allowed to expand to near confluence, reaching approximately 3 million cells per flask. After reseeding, each group was exposed to Etoposide for one week at increasing concentrations: 0.5 μM (group A), 1.0 μM (group B), and 5.0 μM (group C). Following treatment, surviving colonies across all 30 independent populations were quantified and individually isolated. Jaffrezou and colleagues exposed each population to varying concentration levels of Etoposide, operating under the principle that if survival were induced by Etoposide exposure, resistance would be fairly uniform across each population over time (1994). However, Jaffrezou's findings were in accordance with the opposite: survival across each flask was completely random with great variance. In this instance, the conclusion was that

the underlying cause behind resistance was most likely due to genetic mutations. More specifically, these genetic mutations were variants that provided a selective advantage in presence of Etoposide, arising spontaneously across all three flasks.

After isolating colonies that showed heightened resistance, the phenotype was verified by substituting Etoposide to doxorubicin, another topoisomerase II inhibitor that works by intercalating within topoisomerase II to disrupt its function and generating toxic free radicals to induce irreparable oxidative stress while preventing DNA repair (Thorn et al. 2011). The results were nearly identical, with the same Etoposide-resistant isolated colonies conferring relatively higher levels of resistance against doxorubicin as well, confirming that spontaneous mutations in the coding region of topoisomerase II are the force driving resistance.

Despite decades of clinical use, the full spectrum of Topo IIα mutations capable of conferring resistance to Etoposide remains undefined. Prior studies have identified select resistance-associated mutations; however, these findings are often limited to individual variants or narrow mechanistic interpretations (Mao et al. 1999, Farsani and Sadeq 2018). As a result, the broader genetic landscape contributing to Etoposide resistance has yet to be fully elucidated. This lack of complete understanding complicates both the prediction of therapeutic success and the design of strategies to overcome resistance, because research and development teams do not know precisely where within the amino acid sequence such mutations are occurring.

Because resistance-conferring genetic alterations are not commonly tested before physicians prescribe a certain drug treatment course, patients may receive Etoposide-based therapies despite harboring tumor populations with reduced drug sensitivity (Ganapathi and Ganapathi 2013). Such mismatches between treatment and tumor genotype lead to diminished efficacy, unnecessary toxicity, and delayed implementation of alternative therapeutic strategies --

extremely detrimental in a cancer treatment plan where time is of utmost importance. Moreover, incomplete characterization of resistance mechanisms constrains efforts to optimize chemotherapeutic drug development and limits insight into how structural and functional changes to the enzyme influence patient outcomes.

Previous experiments have aimed to further this cause-and-effect relationship between the genetic makeup of topoisomerase and its activity in the presence of topoisomerase inhibitors. One particular experiment synthesized a double mutant with two known mutations conferring Etoposide resistant – arginine mutating to glutamine at the 450 base pair position and proline mutated to serine at the 803 base pair position (R450Q and P803S) – to assess if a gene encoding for Human Topoisomerase IIα containing both mutations would display greater resistance against Etoposide, thereby leading to decreased drug efficacy and higher likelihood of adverse effects for the patient (Hsiung et al. 1996). The research team found significantly higher resistance levels compared to the unmutated Human Topoisomerase IIα. Further, these mutations of R450Q and P803S were confirmed in clinical samples of patients expressing resistance to Etoposide (Mao et al. 1999). Others have explored the opposite effect, referred to as "S phase cytotoxicity", and the examination of amino acid mutations that render Human Topoisomerase IIα more susceptible to Etoposide treatments (D'Arpa and Liu 1989). This discovery is also beneficial to treatment teams, as it allows them to discern which medications are best fit for certain patients, as opposed to solely understanding which medications are likely to present as ineffective measures.

Experimental Objective

The objective of the present study was to investigate the genetic drivers underlying resistance to Etoposide, with emphasis on alterations affecting Human Topoisomerase IIα

function. Using a directed evolution approach, we pursued three distinct aims: (1) generate a diverse library of TOP2A mutations using error-prone PCR and *in vivo* homologous recombination, (2) apply selective pressure with Etoposide to enrich for drug-resistant variants, and (3) identify and quantitatively characterize resistance-conferring mutations through sequencing and dose-dependent survival assays. Our study aimed to contribute to a more mechanistic understanding of one of the most common chemotherapy failures, and to inform future efforts toward precision-guided cancer treatment.

Our experiment differs from such previous experiments due to the use of random mutagenesis as a means of forcefully inducing mutations. Rather than testing specific mutations and assessing their proficiency, our experiment calls upon error prone polymerase chain reaction (PCR) to induce random changes into the coding region, of which the exact change is unknown until after the screening against the Etoposide. While meaningful, the targeted approaches of (Hsiung et al. 1996) and (D'Arpa and Liu 1989) may overlook unexpected or distal residues that contribute to resistance through allosteric or conformational effects. An unbiased selection strategy such as error prone PCR has the potential to reveal novel resistance-conferring mutations that otherwise would not be predicted.

Success would be defined by obtaining single-site substitutions that demonstrate increases in survival relative to the unmutated, "wild-type" Human Topoisomerase IIα gene across multiple drug concentrations, thereby expanding the current map of Topo IIα residues capable of mediating Etoposide resistance. By integrating mutagenesis with phenotypic quantification, this approach seeks to extend prior targeted studies and provide a broader functional landscape of Topo IIα resistance determinants.

Methods

Materials

Saccharomyces cerevisiae yeast plasmids, yeast strains, and oligosequences were generously provided by the Nitiss laboratory at the University of Illinois. The following plasmids were obtained for gap-repair and control experiments: pMJ1 (complete gene Wild Type control), pGap1, pGap2, pGap, and pGap4 each containing deliberate deletions between designated amino acid regions. Figure 5 outlines the regions of each designed plasmid's exact amino acid gap location, synthesized via inverse PCR, meaning the entire plasmid region was amplified with the exception of the region of the desired gap. Yeast strain YMtt, a cell line containing a temperature sensitive yeast topoisomerase prohibiting growth at 25°C, was also obtained from the Nitiss laboratory.

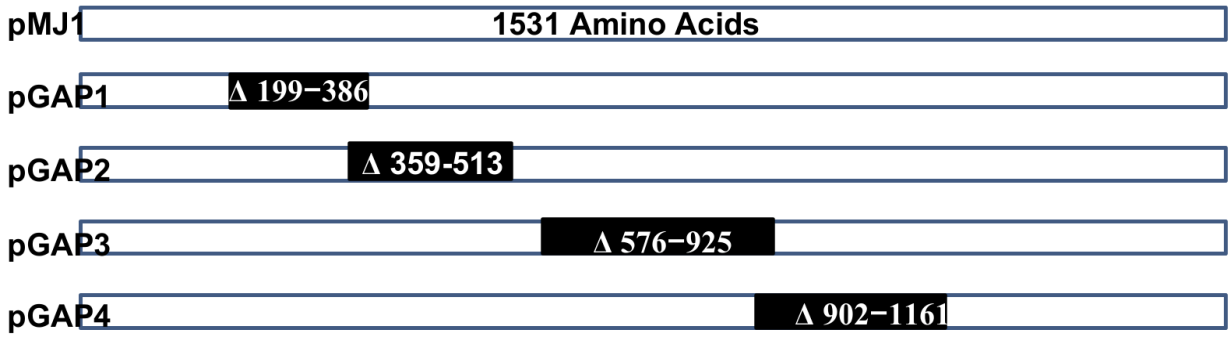

Figure 5 Gap breakdown by amino acid regions. Black regions show excluded regions of inverse PCR, effectively creating a plasmid with a "gap" between the designated amino acid locations (adapted from Bayne 2023).

Alongside the Nitiss laboratory, all oligonucleotides used for cloning, error-prone PCR, and sequencing were purchased from Invitrogen. Etoposide used in yeast selection assays was

obtained from ChemDirect. The R450Q positive-control plasmid was synthesized by GenScript. The workflow of the first phase, utilizing each of these materials, of our study is represented in Figure 6.

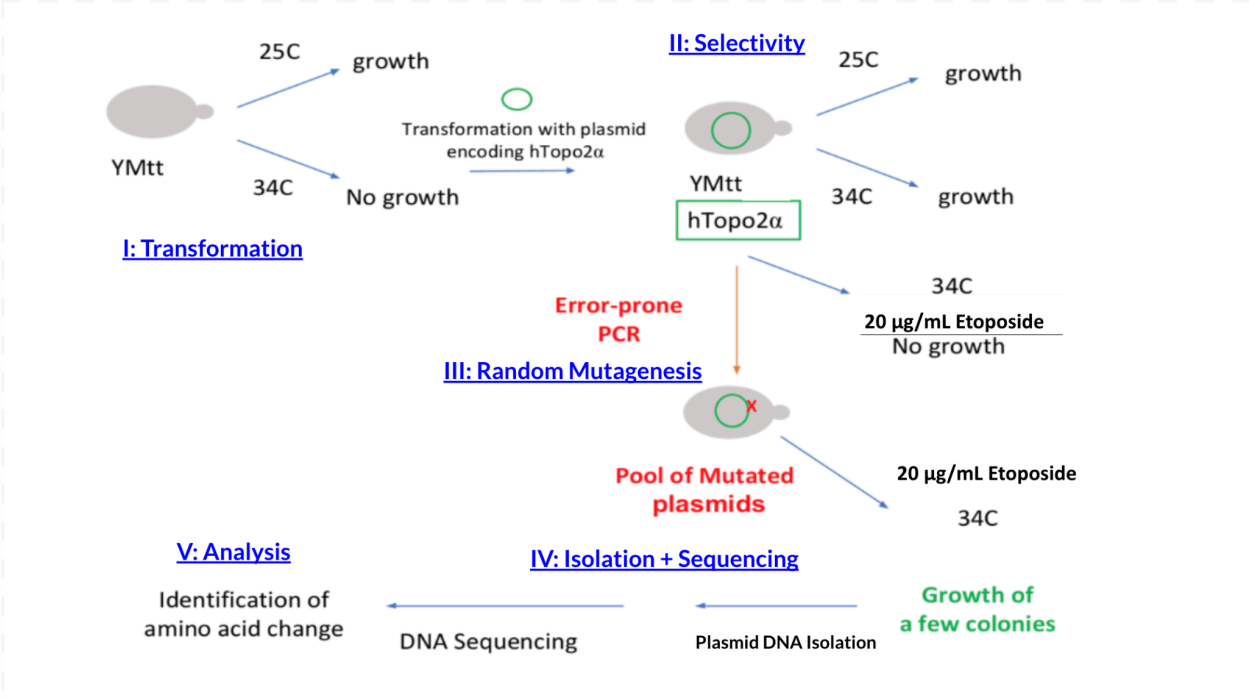

Figure 6 Workflow of Phase I. Maps all steps from transformation until DNA sequencing. (Adapted from Bayne 2023).

Transformation and Selection

The temperature-sensitive yeast strain YMM10t 2-4, which carries a defective endogenous TOP2 allele and is unable to grow at the non-permissive temperature of 34 °C, was used for all selection experiments. A yeast plasmid expression construct, designated pMJ1, containing the human TOP2A coding sequence, was obtained from Dr. John Nitiss and Dr. Karin Nitiss of the University of Illinois Cancer Center. The pMJ1 construct (Figure 7) includes the URA3 selectable marker for growth on uracil-deficient (URA-) media, the human TOP2A gene

under control of the TOP1 promoter, bacterial ampicillin resistance gene (Amp), origin of replication (ori) sequence for propagation in *E. coli* and *S. cerevisiae*, multiple restriction sites for cloning, and a lacZ region. In addition, four gap-repair plasmids (pGap1-4), constructed through inverse PCR, spanning distinct regions of TOP2A were obtained and used for mutagenesis via *in vivo* homologous recombination.

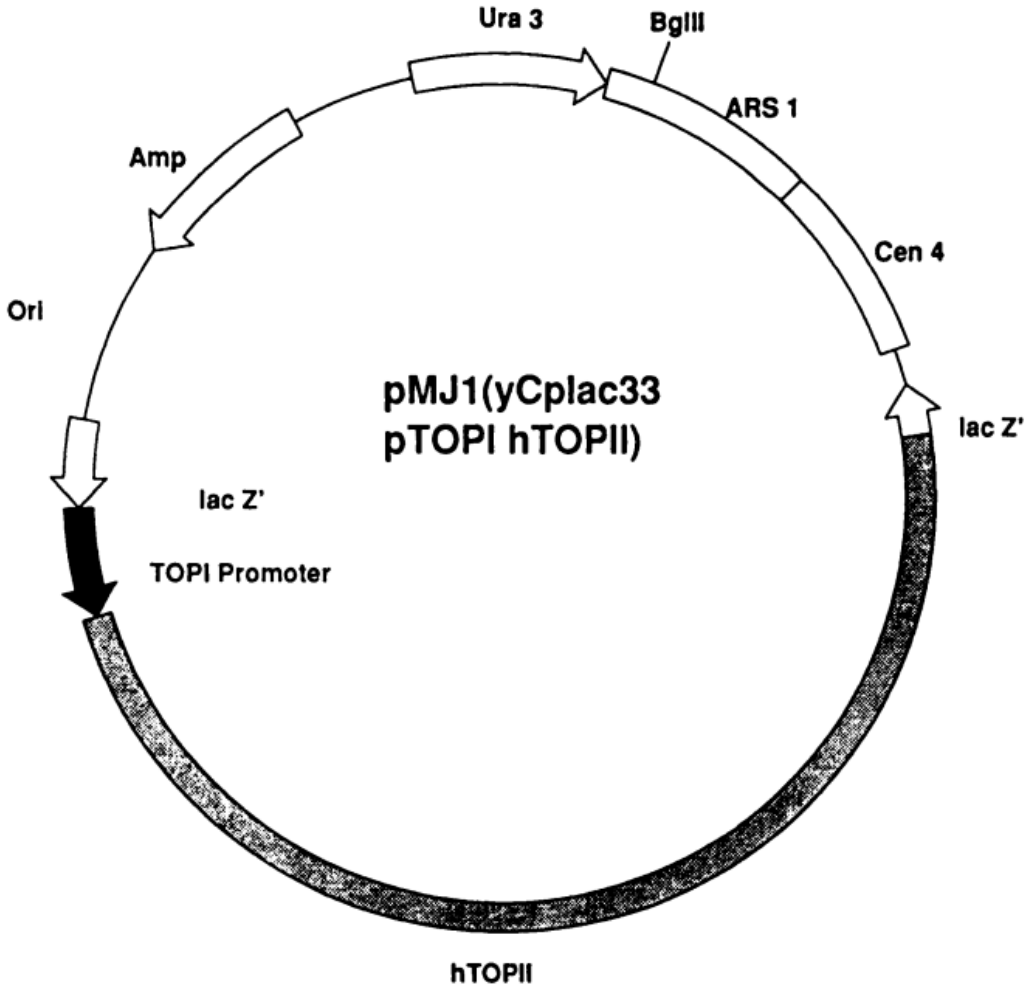

Figure 7 Annotated map of pMJ1. Our yeast plasmid has a Autonomously Replicating Sequence, URA3 marker, CEN origin, promoter, terminator, and cloning sites (Hsiung et al. 1996)

The pMJ1 plasmid was transformed into a temperature-sensitive *S. cerevisiae* yeast strain YMtt using a lithium acetate (LiAc)/polyethylene glycol (PEG) transformation protocol adapted from the Singer Lab at UC Davis ("Yeast Transformation Protocol" 2002). Exponentially growing cultures were harvested at Optical Density (at 600 nm) values between 0.5 and 1.1, pelleted at 3,000 rpm for 5 minutes, and washed in 1x Lithium Acetate/Tris-EDTA (LiAc/TE) buffer. Cells were resuspended in LiAc/TE and aliquoted into microcentrifuge tubes. For each transformation, plasmid DNA was combined with denatured carrier DNA derived from salmon sperm from our transformation kit. A freshly prepared PEG/LiAc solution was added to facilitate DNA uptake, followed by incubation at room temperature for 1 hour. Dimethyl sulfoxide (DMSO) was added prior to heat shock at 42°C for 5 minutes to promote membrane permeability. Serial dilutions were prepared and plated onto URA^- selective media. Plates were incubated at 25°C to allow colony formation, followed by incubation at 34°C for selection under non-permissive conditions.

Random Mutagenesis

Random mutagenesis of the human TOP2A coding sequence was performed using the GeneMorph II Random Mutagenesis Kit (Agilent Technologies) according to the manufacturer's instructions. Mutation rate was regulated by adjusting the initial template concentration per 50 µL reaction, with template quantities selected to achieve a low mutation frequency range (0 - 4.5 mutations per kilobase).

All PCR reactions were assembled on ice. Each 50 µL reaction contained 31 µL nuclease-free water, 5 µL of 10x Mutazyme II reaction buffer, 1 µL of 40 mM dNTP mix, or an aqueous solution containing the four nucleotides in equimolar concentration (200 µM final

concentration of each nucleotide), 2 µL primer mix obtained from Thermo Fisher Scientific (all primer mix combinations are described in Appendix A), 1 µL Mutazyme II DNA polymerase (2.5 U/µL), and 10 µL of 1.2 µg pMJ1 template DNA containing the target TOP2A region (Agilent Technologies 2015). Different primer combinations were used for different gap mutagenesis reactions. Reactions were gently mixed, briefly centrifuged to collect contents, and immediately placed into a thermocycler.

PCR amplification was performed using the following cycling parameters: an initial denaturation at 95 °C for 2 minutes, followed by 30 cycles consisting of denaturation at 95 °C for 30 seconds, annealing at a temperature 5 °C below the calculated primer melting temperature for 30 seconds (55°C), and extension at 72 °C for 30 seconds per kilobase of target sequence. A final extension step was performed at 72 °C for 10 minutes to ensure complete amplification of all products.

Upon completion of thermocycling, 10 µL of each PCR reaction was analyzed on a 1% agarose gel using 1x TE Buffer alongside 5 µL (100 ng) of a 1.1 kb DNA ladder standard (Agilent Technologies 2015). Agarose gel electrophoresis was performed to verify PCR amplification of the expected fragment size. Band intensity was evaluated to confirm adequate amplification prior to downstream applications.

PCR products were purified using the Monarch PCR & DNA Cleanup Kit (New England Biolabs 2021) according to the manufacturer's protocol. Binding buffer was added to each reaction, before samples were loaded onto purification columns, washed to remove residual primers, nucleotides, salts, and polymerase, and eluted in 20 µL nuclease-free water. DNA concentration and purity were assessed using spectrophotometric analysis. Samples exhibiting

concentrations between 40 - 60 µg/mL via NanoDrop™ spectrophotometry and acceptable A260/A280 ratios were retained for subsequent applications.

For library construction, purified mutagenized PCR fragments were transformed into yeast together with a linearized, gapped pMJ1 expression vector. Homologous recombination within yeast cells facilitated *in vivo* gap repair, resulting in reconstitution of a complete pMJ1 plasmid containing randomly introduced mutations within the targeted region of human TOP2A gene. This approach enabled direct incorporation of mutagenized fragments into the yeast expression system without intermediate *in vitro* ligation (Agilent Technologies 2015).

Repaired plasmids were maintained in a temperature-sensitive yeast strain, Ymtt, lacking functional endogenous topoisomerase II activity at the non-permissive temperature. Transformants were selected on uracil-deficient (URA^-) media, and were incubated under selective conditions to ensure plasmid retention and functional expression of Human Topoisomerase IIα variants for downstream phenotypic screening.

Screening

Transformed yeast colonies containing mutagenized pMJ1 plasmids were initially screened by replica gridding onto control uracil-deficient (URA^-) agar plates. Plates were incubated at 34°C, the restrictive temperature for the temperature-sensitive yeast strain. A schematic representation of the gridding methodology is shown in Figure 8a. R450Q was used as a positive control, understanding that it is a resistance-conferring mutation against Etoposide, while pMJ1 with unmutated TOP2A gene represents a negative control, understanding that Etoposide should exert its effects on the wild-type form of the enzyme. Growth at 34°C indicates functional complementation by the mutagenized hTOP2A construct, whereas absence of growth

is consistent with nonsense mutations, frameshift mutations, or deleterious missense mutations that restrict Topoisomerase II activity. Colonies failing to grow under these conditions were excluded from further analysis. This initial selection step ensured that only colonies expressing catalytically functional Topoisomerase II variants were retained for downstream drug sensitivity screening.

Colonies demonstrating growth on URA$^-$ plates at 34°C were subsequently transferred to URA$^-$ plates supplemented with increasing concentrations of the topoisomerase II inhibitor Etoposide (0, 10, and 50 µg/mL). Colonies were gridded in an identical spatial arrangement across all drug concentrations to enable direct comparison of growth phenotypes, as well as on progressively increasing concentrations of Etoposide (Figure 8b). Plates were incubated at 34°C for 24 hours prior to analysis.

a)

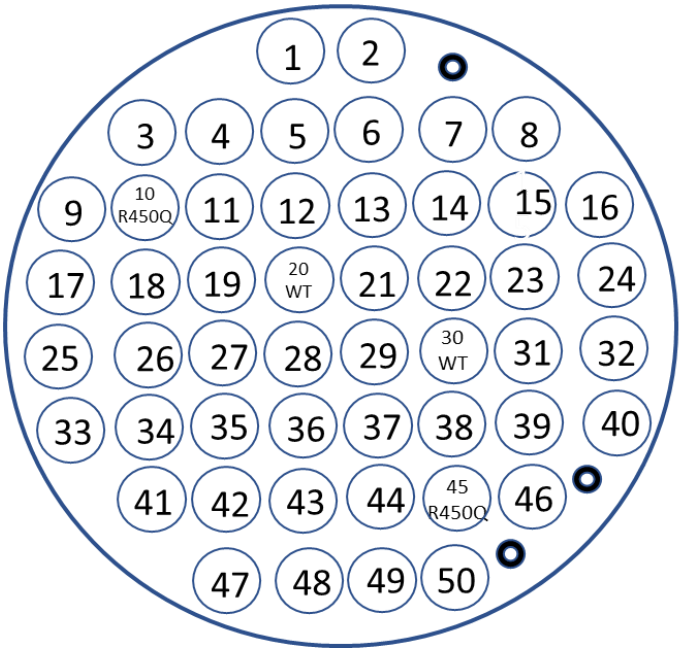

b)

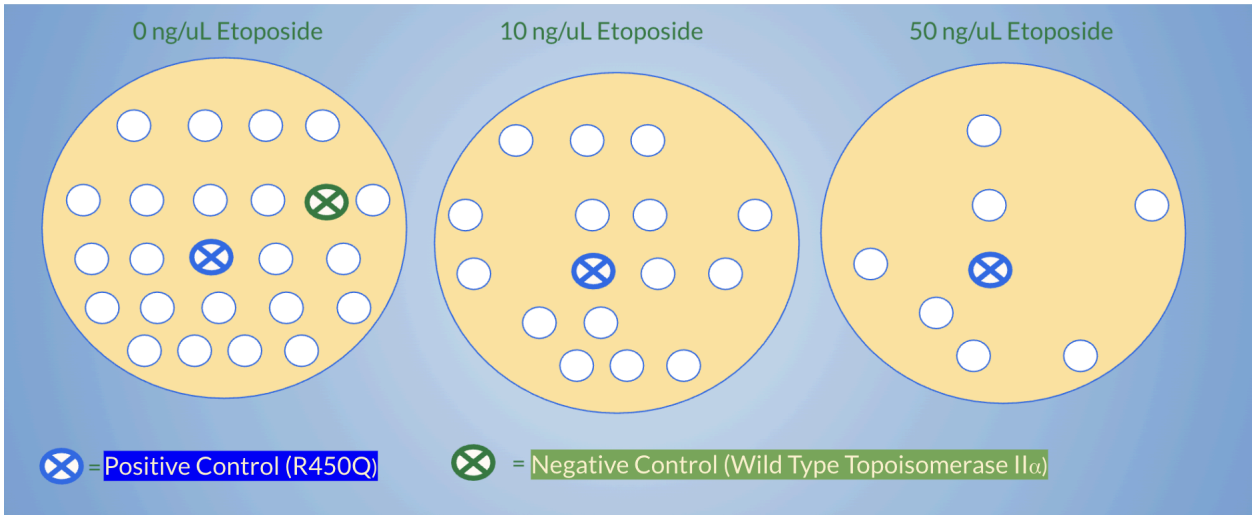

Figure 8 Screening process on URA- plates a) single plate layout of 50 sample colonies with allotted locations for positive control R450Q and negative control WT. b) Progressive plate screening assay with differing Etoposide concentrations to select colonies for DNA sequencing analysis.

Plasmid Isolation and Purification

To verify the presence and integrity of the mutagenized hTOP2A region, PCR amplification was performed using high-fidelity Q5 2x Master Mix (New England Biolabs 2021). Each 50 µL reaction contained 10 µL of extracted plasmid DNA, 25 µL Q5 2x Master Mix, 4 µL each of forward and reverse primers, and nuclease-free water to final volume. PCR amplification was performed under conditions optimized for primer annealing and fragment length. Sequences for primers are provided in Appendix A.

Amplified products were analyzed by 0.8% agarose gel electrophoresis in 1x TAE Buffer to confirm successful amplification – confirmed by band intensity – and expected fragment size, verified by the band's location on the gel. PCR products were subsequently purified using the Monarch PCR & DNA Cleanup Kit (New England Biolabs 2021) to remove residual primers,

nucleotides, enzymes, and salts. Purified DNA concentration and purity were reassessed via NanoDrop spectrophotometry prior to sequencing.

Sequencing

Purified PCR products were diluted to a final concentration of 3 ng/mL to optimize sequencing quality and prevent signal suppression associated with excessive template input. Sequencing reactions consisted of 10 µL of PCR product (30 ng/mL) and 5 µL of 5 µM sequencing primer. Sequencing primers are listed in Appendix A. A specific subset was used for each Gap plasmid product used to ensure complete coverage of the amplified region. Each primer's sequence is presented in the Appendix.

Reactions were sent to GeneWiz for Sanger sequencing. Results were delivered in the form of Applied Biosystems Files, which were loaded onto Thermofisher to generate sequence data. Sequencing data were analyzed by alignment against the reference hTOP2A sequence derived from the pMJ1 plasmid construct. Nucleotide alignments were performed using the National Center for Biotechnology Information Basic Local Alignment Search Tool (NCBI BLAST) to identify deviations from the wild-type reference sequence. Observed nucleotide substitutions were documented, including precise base position and codon location.

To determine whether nucleotide substitutions resulted in amino acid changes, BLASTx analysis was performed to translate the nucleotide sequence and compare the predicted protein sequence to wild-type Topoisomerase IIα. Amino acid substitutions were identified and evaluated for potential functional relevance based on their position within the coding sequence. Particular attention was given to substitutions occurring within known functional domains or conserved regions of the protein.

Identified amino acid substitutions were categorized based on biochemical properties, including polarity, charge, and predicted structural localization. These classifications were used to assess potential structure-function relationships and to evaluate whether specific residue changes could contribute to altered drug sensitivity.

Quantification of Etoposide Resistance

Previously frozen yeast strains possessing individual mutant hTOP2A plasmids were thawed and inoculated into 10 mL of URA^- liquid media. Cultures were incubated overnight at 34°C with shaking to ensure logarithmic growth. After 24 hours OD_{600} measurements were obtained to assess culture density.

To standardize inoculum density across all mutants, each overnight culture was diluted to an OD_{600} of 0.12 in 20 mL of fresh URA^- media. Diluted cultures were incubated for an additional 24 hours at 34°C with shaking to ensure uniform opportunity for growth prior to plating. Each overnight culture was grown overnight in varying levels of Etoposide (0 µg/mL, 10 µg/mL, 30 µg/mL, 100 µg/mL, and 300 µg/mL), in preparation for subsequent on fresh URA- plates.

Following incubation, 500 µL aliquots were prepared from each culture, and serial ten-fold dilutions (10^0, 10^{-1}, 10^{-2}, 10^{-3}, and 10^{-4}) were generated in sterile URA^- media. From each dilution, 16 µL was plated onto rectangular URA^- agar plates (Fazen plates) containing the designated Etoposide concentration. Plates are referred to as Fazen plates because the idea to plate several dilutions on one plate was obtained from the Fazen laboratory at Drew University. Samples were arranged in columns corresponding to dilution factor to facilitate direct comparison. Plates were incubated at 34°C for 48 - 72 hours, after which individual colonies were enumerated manually. Colony Forming Units per milliliter, or CFU/mL was calculated by

multiplying each colony count by its dilution factor, then by 62.5 to receive a final count in terms of 1000 uL.

Once all colony counts were standardized in CFU/mL, we utilized Microsoft Excel to graph survivorship curves for each mutant. Some particularly noteworthy curves were overlaid onto graphs of the Wild-Type to further highlight the degree of resistance.

Mutants demonstrating sustained colony formation at higher drug concentrations (30 μg/mL, 100 μg/mL, and 300 μg/mL) were selected for further quantitative analysis.

Further analysis utilized a similar workup as the secondary screening, but instead involved plating 100 μL onto circular URA- plates referred to as "big plates." Like the Fazen plates, colonies were grown up in 10 mL of URA- media, each with a corresponding value of Etoposide (0 μg/mL, 10 μg/mL, 30 μg/mL, 100 μg/mL, and 300 μg/mL), in preparation for subsequent on fresh URA- plates. The 14 colonies showing the most heightened resistance at higher Etoposide concentration levels were selected for this advanced screening. All colonies were plated in duplicate, and the average colony counts of both plates were converted into CFU/mL at each Etoposide concentration were designated as each respective mutant's "final count." CFU/mL was calculated by multiplying each colony's average count among its two plates by its dilution factor, then by 10 to standardize our 100 μL sample count to 1 mL.

Mapping on 3-Dimensional Model

Structural modeling of Human Topoisomerase IIα was performed using the online molecular visualization software PyMOL to visualize the locations of discovered resistance-conferring mutants in relation to Etoposide binding residues, the enzyme's catalytic domains, and other potent mutants identified in this study. A structural model of Topoisomerase IIα bound to DNA and Etoposide was imported into PyMOL and used as the template for

analysis. Discovered mutants were mapped onto the protein structure and individually highlighted to determine their spatial relationship to the Etoposide binding pocket and surrounding catalytic regions. Bound Etoposide was highlighted in yellow, Etoposide binding residues in purple, the R487I mutant in blue, and the remaining 13 potent non-R487I mutants in orange to allow clear visualization of structural organization and clustering patterns. Additional comparisons between potent mutants were performed to assess whether resistance-conferring substitutions localized to shared structural regions within the enzyme. Generated structural models were used to evaluate how mutation positioning may contribute to altered Etoposide interaction and resistance phenotypes.

Results

Validation of Yeast Complementation System

Successful uptake of the Human Topoisomerase IIα gene from the pMJ1 vector was assessed by growth at 34 °C, a temperature at which endogenous yeast topoisomerase is inactive. While both yeast and human topoisomerase supported growth at 25 °C, only colonies expressing Human Topoisomerase IIα exhibited growth at 34°C because of the temperature-sensitive property of our YMtt yeast topoisomerase prohibiting growth at 34°C. Figure 9a represents this distinction, showing the variation in growth success between pMJ1 and Ymtt at both 25°C and 34°C.

a)

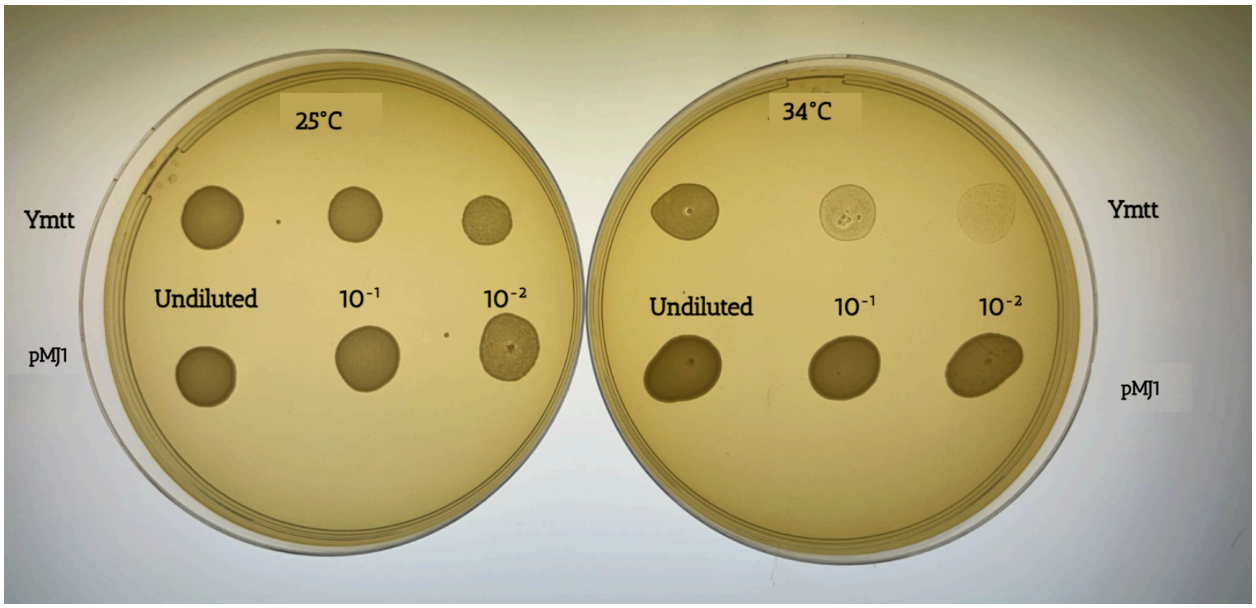

b)

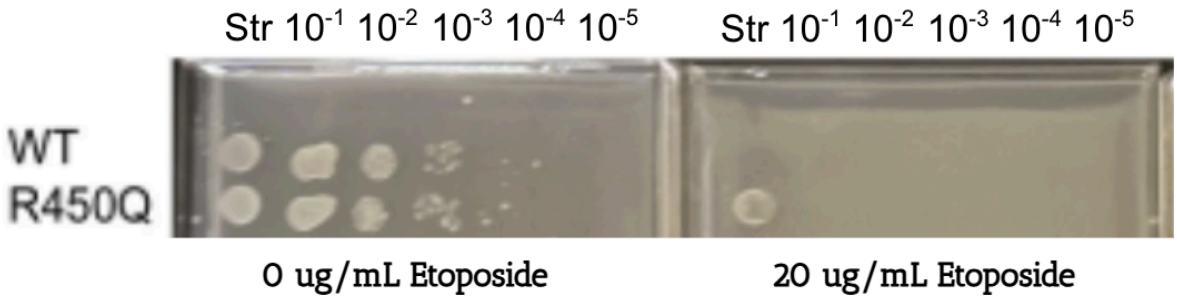

Figure 9 Ymtt vs. pMJ1 plating at 25°C and 34°C and validation of positive and negative controls. a) Left plate represents undiluted, 10^{-1} dilution, and 10^{-2} dilution of both Ymtt with yeast topoisomerase and pMJ1with Human Topoisomerase IIα at 25°C. Right plate represents the same array, but at 34°C. All other conditions were kept constant. b) Validation of positive control R450Q and negative control WT pMJ1 in their respective abilities to express resistance and susceptibility to Etoposide. Str stands for "straight", or an undiluted plating.

Generation and Identification of Resistant Variants

Error-prone PCR was used to generate a mutagenized library of Human Topoisomerase IIα variants; the variants were introduced into yeast and subjected to functional selection for altered Etoposide response. Upon completion of transformation with the appropriate gap and PCR product, transformants from each gap were subject to plating on agarose URA- plates containing 10 μg/mL and 20 μg/mL Etoposide. Resistant clones identified in this primary screen were subsequently sequenced to determine the underlying genetic changes.

Figure 10 represents the amplification of the Gap1 and Gap4 regions on a 0.8% agarose gel. We expected pGap1 to yield a band at 671 base pairs, pGap2 to yield a band at 714 base pairs, pGap3 to yield a band at 1217 base pairs, and pGap4 to yield a band at 1036 base pairs. All 4 gaps were necessary to ensure distribution of induced mutations across the entire genome. The error prone PCR product should correlate with these values in base pairs. Gel electrophoresis assay showed alignment with ~650 base pairs for our mutated Gap1 plasmid, with alignment at ~1100 bp for the mutated Gap4 plasmid, both in line with our expected results.

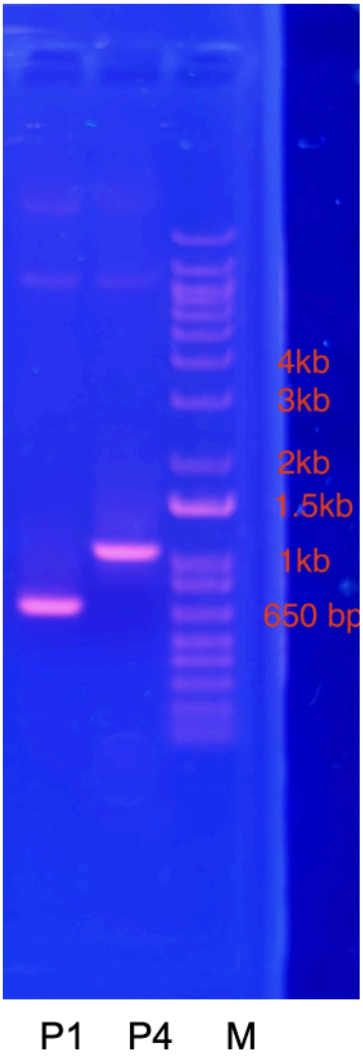

Figure 10 Results of an agarose gel with 1x TE buffer following error prone PCR of GAP1 and GAP4 plasmids. P1 corresponds to pGap1insert while P4 represents the pGap4 insert. M represents the marker that is used as a reference scale to determine the size.

Wild Type Etoposide Sensitivity

Colonies exhibiting growth at 34 degrees Celsius were determined to possess active Human Topoisomerase IIα genomes following transformation with pMJ1. Replica plating technique was utilized to ensure identical placement of colonies along with consistency in amount plated. Sample progressive screening from 0 µg/mL to 20 µg/mL Etoposide is shown in Figure 11. Colonies showing growth at the higher concentrations of the drug were determined to have more robust resistance.

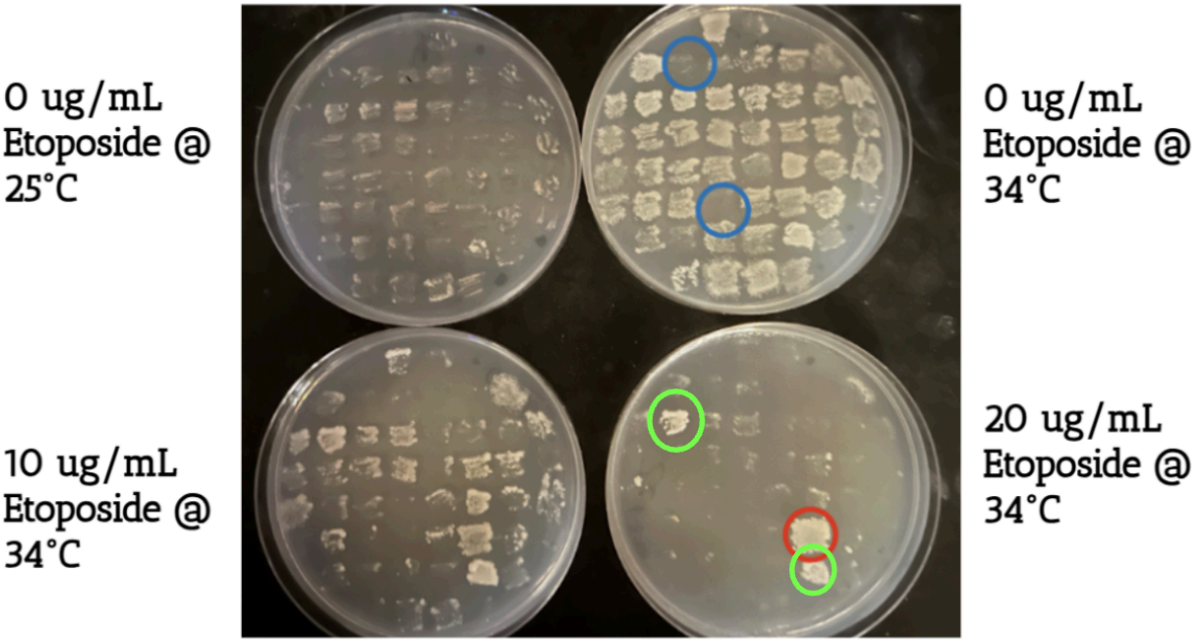

Figure 11 Representative screening plate from Gap 1. Blue circles represented putative inactive mutations, while the red circle represented a sample robust mutation, or a mutation conferring notable resistance against Etoposide. Green circles show positive control R450Q.

Figure 11 displays the disparities in growth for Gap 1 mutations at increasing concentration of Etoposide. Plate 1 (Top Left) shows the source plate from which the colonies

were selected. Replica plating allowed these colonies to later be transferred to three succeeding plates, each with a different concentration of Etoposide: 0 μg/mL (Plate 2: Top Right), 10 μg/mL (Plate 3: Bottom Left), and 20 μg/mL (Plate 4: Bottom Right). Though sequencing data was not readily available, results from screening plates such as the ones presented in Figure 12 allow us to discern which colonies to select for further analysis via Sanger Sequencing.

This process was repeated for Gaps 2, 3, and 4, culminating in 121 unique clones successfully advancing to DNA sequencing. In the Figure 11 subset, the majority of colonies experienced decline in growth from Plate 2 to Plate 4, or from 0 μg/mL to 20 μg/mL. However, blue circles around clones 4 and 36 on Plate 2 represented putative inactive variants based on temperature-sensitive growth profiles, which were classified as mutations that conferred mutations inactivating the function of Topoisomerase IIα. Plate 3 represented Etoposide resistant mutants at clone 38 (red circle) directly above our plated positive control R450Q, conveying the successful introduction of a mutation conferring strong resistance against Etoposide. In total across all four gaps, we discovered 121 putative Etoposide resistant mutants showing similar phenotype to clone 38. All sets of putative inactive mutations were excluded from advancement to error prone PCR as we discerned that their accumulated mutations have no effect on weakened Etoposide function. Plasmids were isolated, PCR-generated, and sequenced as described in the Methods.

Sequencing

Completion of DNA sequencing revealed 121 isolated colonies across all 4 gaps. Among these, 96 colonies possessed unique mutations while 25 were repeat occurrences. Among the 96 unique colonies, 56 were single mutations which advanced to the second Etoposide screening, while 40 possessed either two or greater than two mutations. Sequencing data were uploaded to

Thermofisher databases in order for complete analysis, and sequence misalignment revealed via NCBI Blast is depicted in Figure 12.

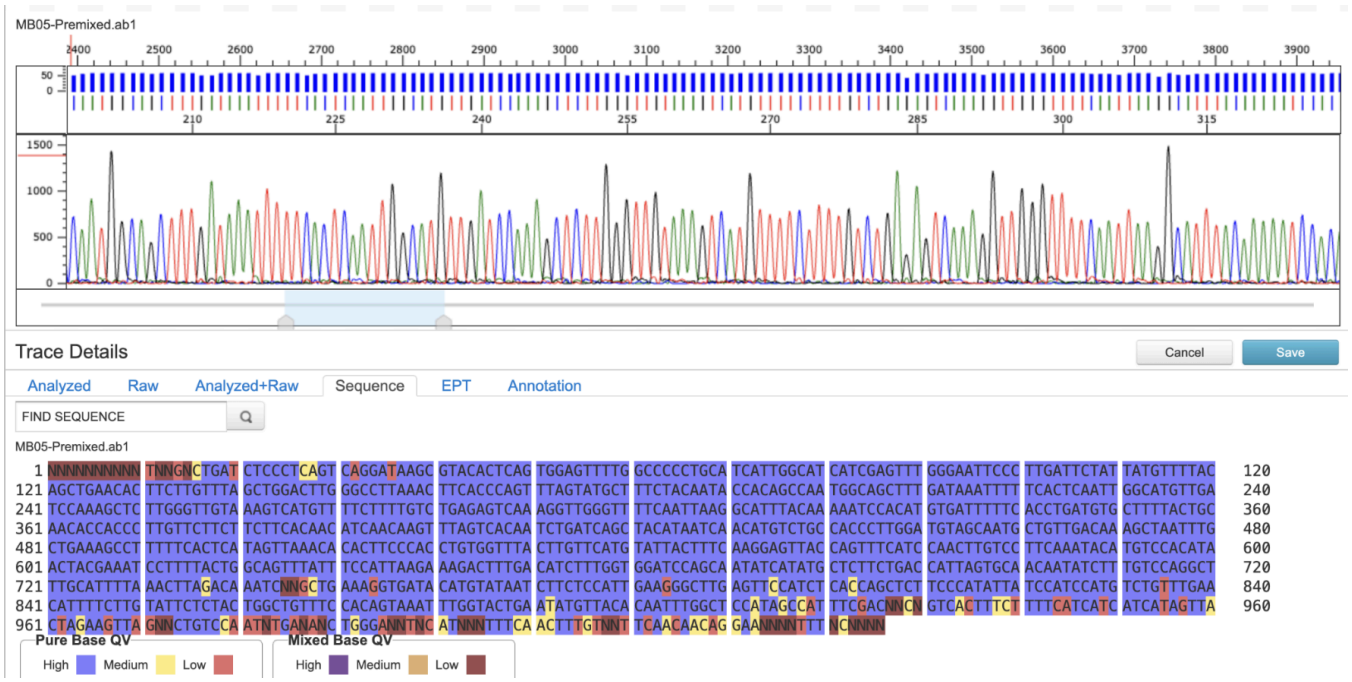

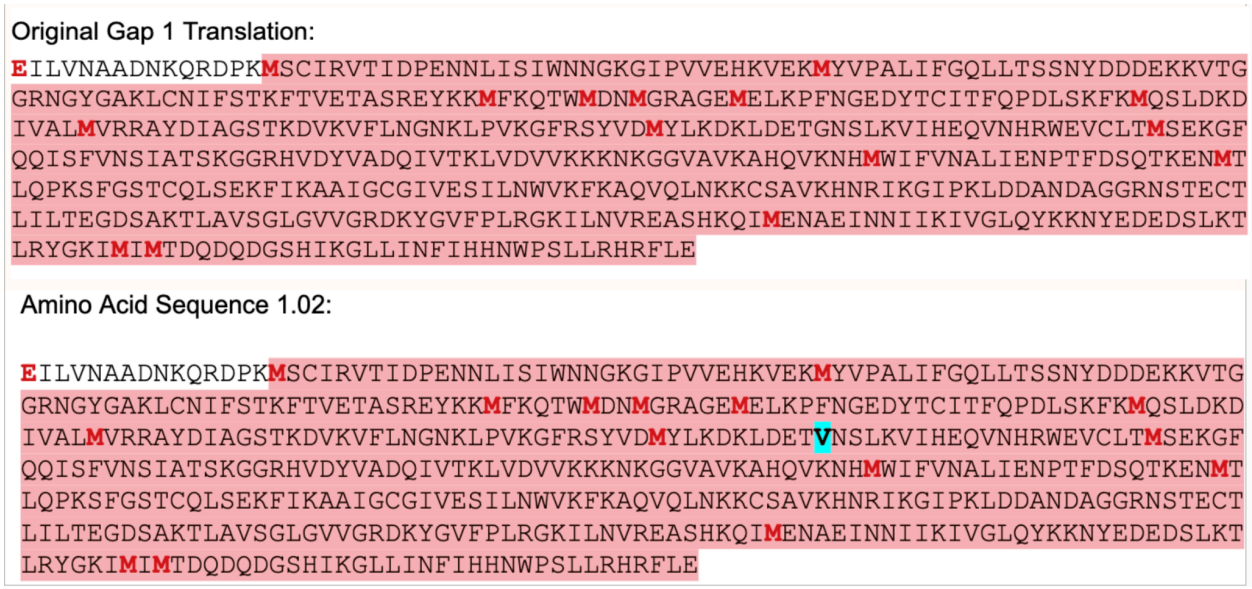

Figure 12 Progression from DNA sequence to mutation identification. Depicts the sequential flow from Applied Biosystem file to Thermofisher to amino acid sequence analysis via NCBI Blast.

Single-nucleotide substitutions were identified by misalignment relative to the wild-type sequence and translated to corresponding amino acid changes. 121 identified mutant variants were subsequently subjected to secondary screening to quantify resistance across increasing concentrations of Etoposide. Mutants exhibiting the highest levels of tolerance were selected for further quantitative characterization. A final, comprehensive list of all discovered mutations is included in Appendix B.

The polarity distribution in Figure 13 shows substitutions between nonpolar residues representing the largest single class, accounting for 57 mutation events. However, alongside a review of the polarity of each amino acid change, our findings also led us to make determinations on localization frequency within the amino acid sequence. Mutations were not evenly distributed across the Topo IIα sequence, but instead were clustered within specific regions. The highest density of mutations were observed between residues 451-600, followed by substantial representation across the 601-900 range. Several positions were recurrently mutated, most notably residue 448, which accounted for 11 independent mutation events, with G448W (Glycine mutating to Tryptophan at the 448 amino acid position) emerging as the most frequently observed individual substitution. Together, these data indicate that Etoposide-resistant variants arise through diverse substitutions that preferentially localize to specific regions of the protein.

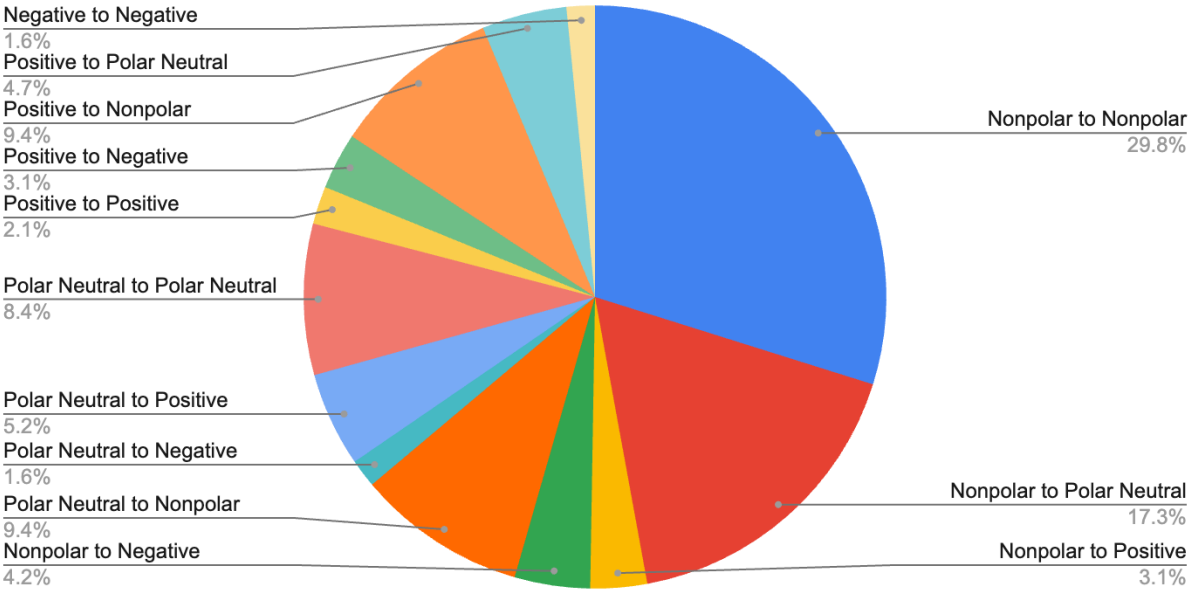

Figure 13 The nature of the polarity change in each discovered mutation from Sanger Sequencing. Sample size of 121 mutation discoveries.

Primary Resistance Screen

Following mutagenesis and sequencing, mutant variants were subjected to a primary resistance screen by growth on Etoposide-containing media. This screen revealed substantial heterogeneity in growth phenotypes, with most colonies exhibiting reduced or absent growth at 34 °C as Etoposide concentration increased, while a subset retained robust growth. Colonies displaying no growth at 34 °C in the absence of Etoposide were classified as inactive and excluded from further analysis. In contrast, colonies exhibiting sustained growth at higher Etoposide concentrations relative to wild-type Human Topoisomerase IIα were classified as putative resistant variants. Figure 14 represents a qualitative examination of our primary resistance screen, observing one set of 10 mutations compared to either positive control R450Q and negative control WT. Colonies displaying viable growth even at or upwards of 30 µg/mL of Etoposide concentrations, allowing us to select them for advancement to the secondary

screening. From all tested sets, the fourteen mutants exhibiting the highest growth at greater than or equal to 30 µg/mL Etoposide were selected for larger-scale plating. These mutants were advanced to secondary quantitative characterization to enable direct comparison of resistance across a broader range of Etoposide concentrations.

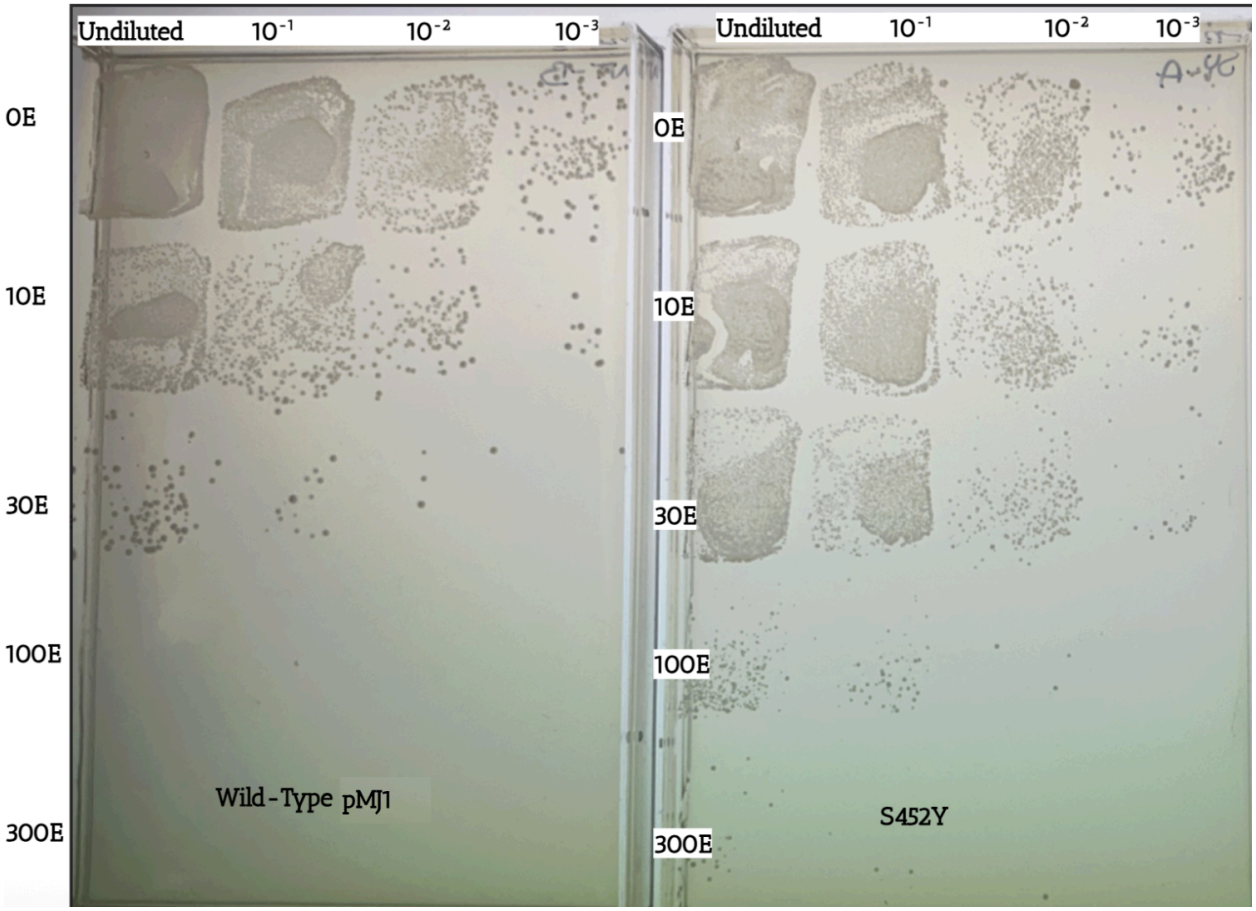

Figure 14 Fazen plate distribution at increasing concentrations of Etoposide. Analysis of growth patterns at 0, 10, 30, 100, and 300 µg/mL of Etoposide. 0E corresponds to 0 µg/mL Etoposide, 10E corresponds to 10 µg/mL Etoposide, etc. Wild-Type pMJ1 is compared side by side to potent Gap 2 mutation Ser452Tyr (S452Y).

Secondary Resistance Screen

Quantitative analysis of colony survival revealed notable dose-dependent differences in Etoposide resistance across the selected Human Topoisomerase IIα variants (Figures 15a and 15b). At 30 μg/mL Etoposide, the majority of mutants exhibited substantially higher survival than wild-type pMJ1, with several variants including R487I, F653S, S452Y, N492S, L491F, I899N, and K798N maintaining survival rates above 75% as compared to <10% for pMJ1. These resistance phenotypes indicate potent resistance under moderate drug pressure. In contrast, wild-type pMJ1 and low-resistance variants such as K1011E and I636T displayed minimal survival at this concentration.

Increasing the Etoposide concentration to 100 μg/mL resulted in a notable divergence in resistance phenotypes (Figure 15b), with overall survival was reduced across all strains and only a subset of mutants retained elevated survival relative to wild type. Notably, R487I exhibited the strongest resistance at the highest drug concentration, while L491F, I899N, and K798N maintained intermediate-level survival, and several mutants that were resistant at 30 μg/mL showed near-wild-type sensitivity at 100 μg/mL, as evidenced in the heat map in Figure 15c. Together, these data demonstrate a wide spectrum of resistance strengths among the selected variants and establish a clear threshold separating high resistant mutants from those exhibiting dose-limited or minimal resistance. Establishing such a threshold creates distinction among the robust mutant group, allowing us to assess the extent to which each mutation affects Etoposide efficacy on a cell population.

a)

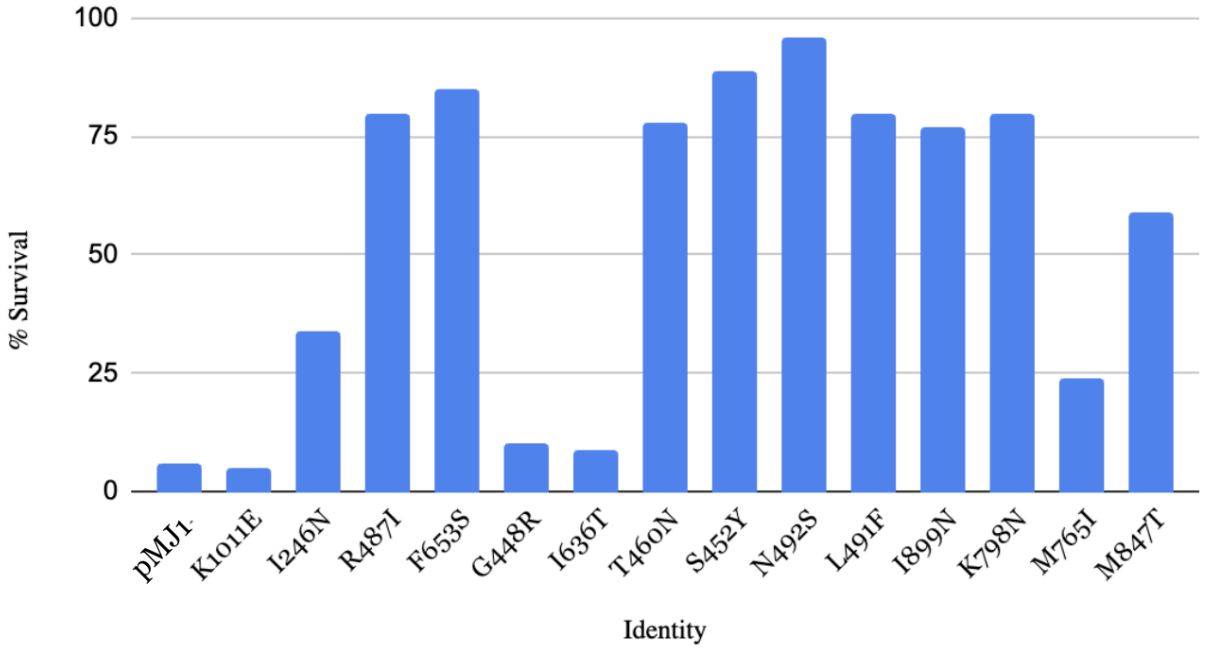
100
75
50
25
0
% Survival
pMJ1-
K1011E
I246N
R487I
F653S
G448R
I636T
T460N
S452Y
N492S
L491F
I899N
K798N
M765I
M847T
Identity

b)

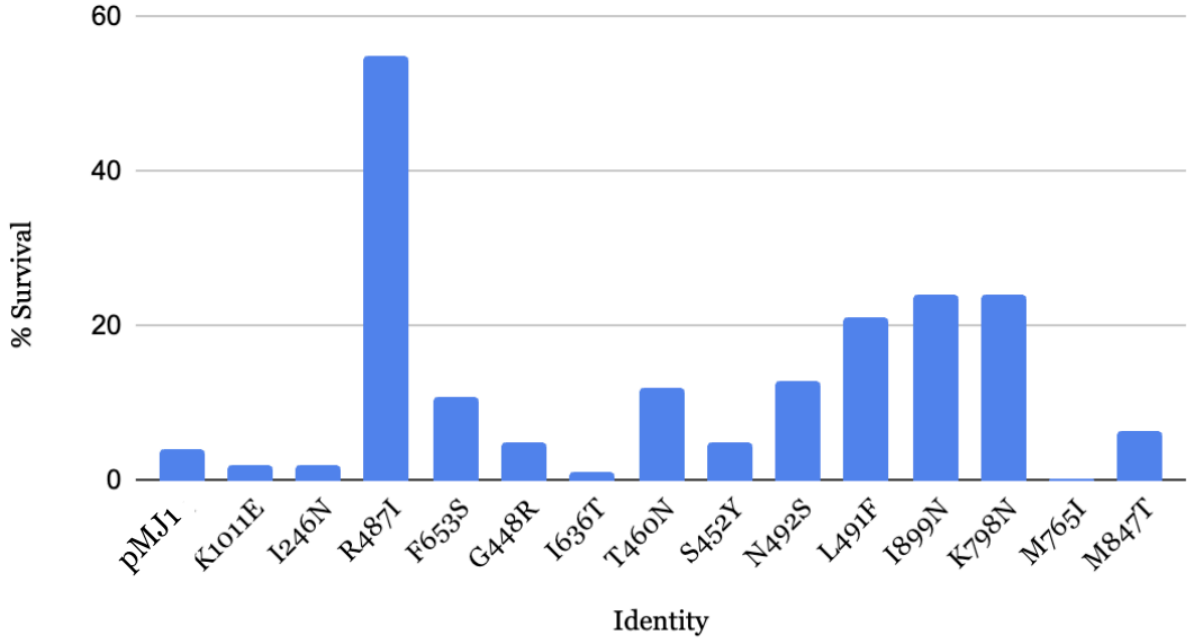
60
40
20
0
% Survival
pMJ1
K1011E
I246N
R487I
F653S
G448R
I636T
T460N
S452Y
N492S
L491F
I899N
K798N
M765I
M847T
Identity

c)

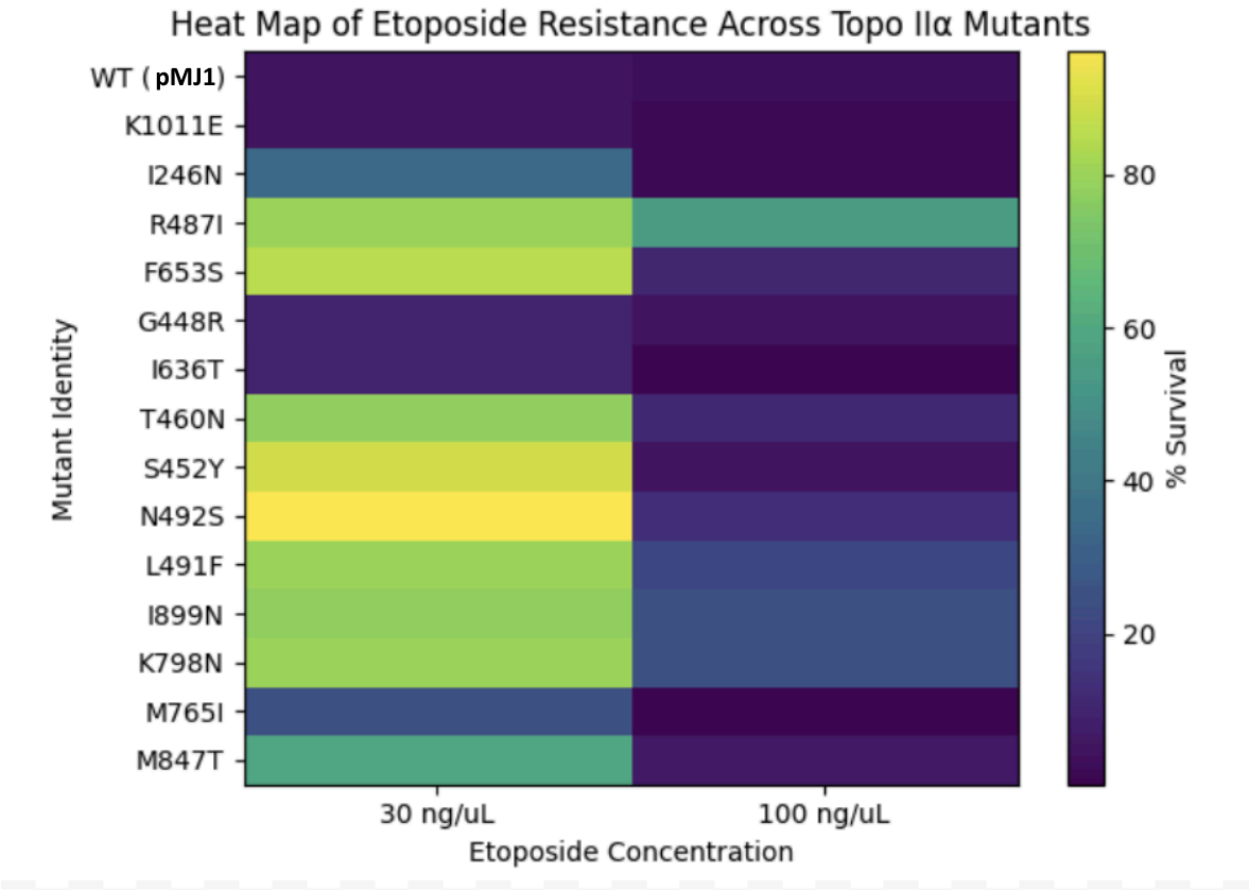

Figure 16 Individual Analyses of 14 most potent mutants a) Respective survival percentage of each mutant at 30 µg/mL b) Respective survival percentage of each mutant at 100 µg/mL of Etoposide c) Heat map of Etoposide sensitivity across 14 selected Topo IIα mutants. Lighter colors (yellow, green, etc.) correspond to higher rates of survival at our two tested values of Etoposide concentration of 30 ng/uL and 100 ng/uL.

Comparative Analysis

Side-by-side comparison of individual mutant discoveries alongside both Wild-Type pMJ1 and other potent mutants were performed in order to assess relative potency. Figure 16

represents a sample comparative analysis between our Wild-Type pMJ1 and discovered Gap 4 mutant M847T. Qualitative observations reveal growth at higher (50 µg/mL and 100 µg/mL) Etoposide concentrations (50 µg/mL and 100 µg/mL) for the mutant M847T where an absence of growth was observed for Wild-Type, indicating a robust resistance-conferring property of the specific discovered mutation. A blend of qualitative and supporting quantitative data from Fazen plate screening assay is highlighted by Figures 17 and 18.

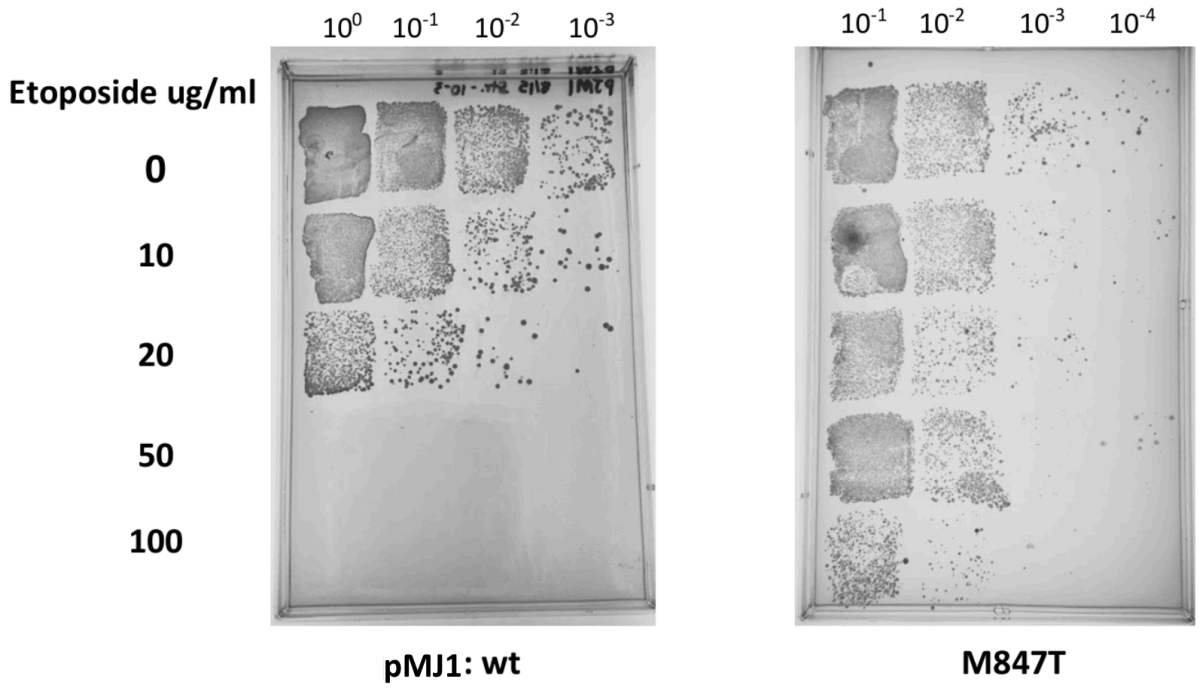

Figure 16 Fazen plate comparative analysis of Wild-Type pMJ1 and mutant M847T. The intensity and density of each region represents colony growth at various dilutions under increasing concentrations of Etoposide.

a)

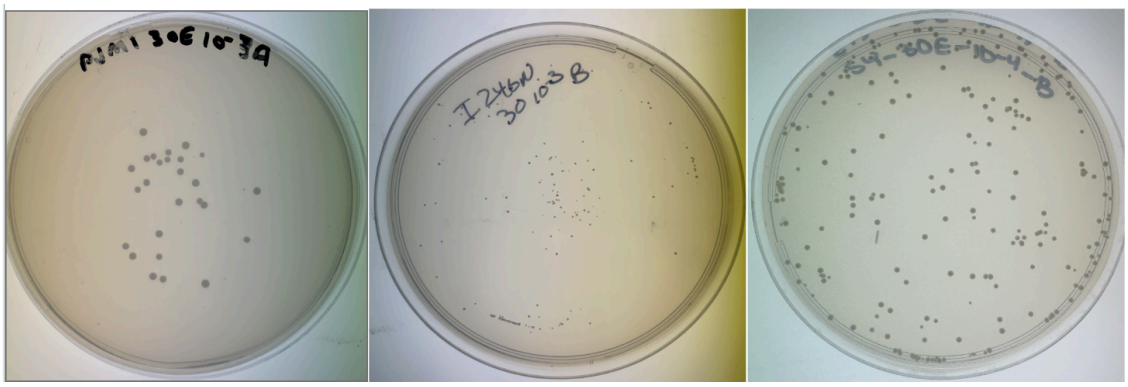

b)

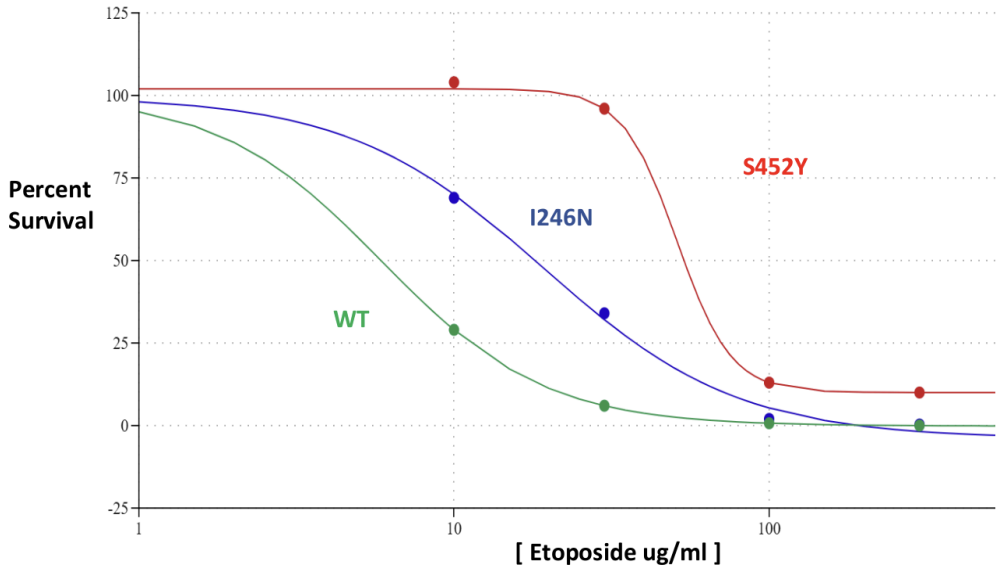

Figure 17 Comparative Analysis Wild-Type pMJ1, I246N, and S452Y mutants. a) Comparative plate analyses of wild-type pMJ1 (10^{-3} dilution), I246N (10^{-3} dilution), and S452Y (10^{-4} dilution) to show variance in colony growth at constant Etoposide concentration of 30 µg/mL. b) Survivorship curve performing colony analysis at 0, 10, 30, 100, and 300 µg/mL. Only plate dilutions with colonies between 30 and 300 were used for this assessment.

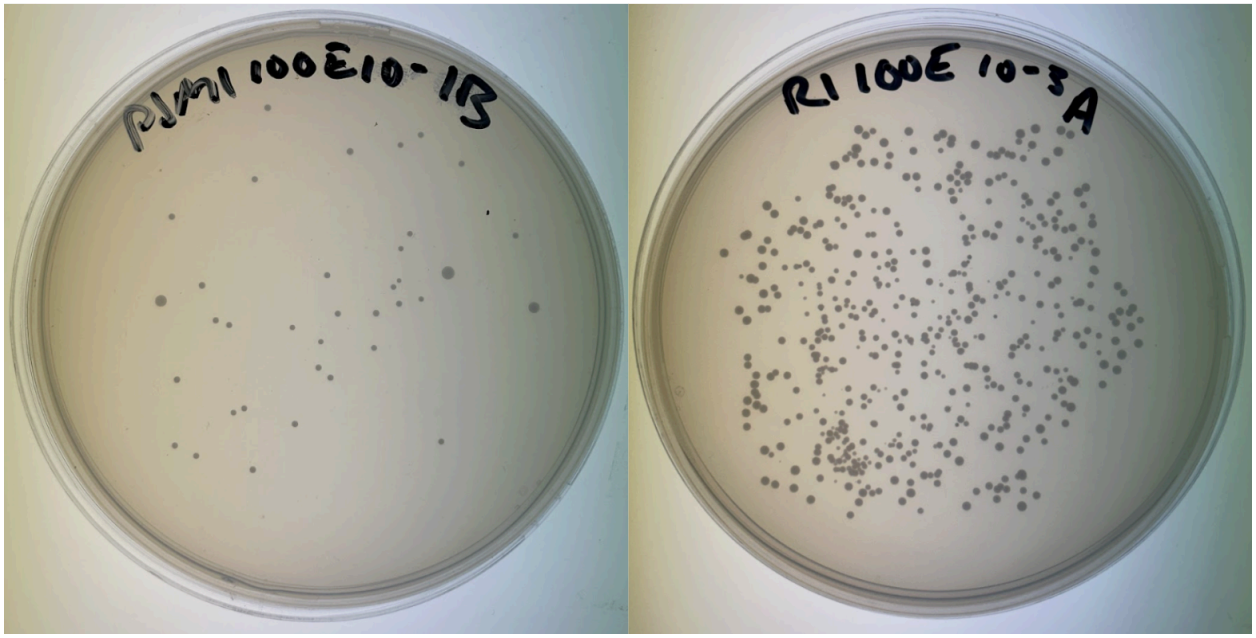

Figure 18 Analysis of Wild-Type pMJ1 and R487I at 100 µg/mL of Etoposide. Both plates were treated with equivalent Etoposide concentrations and given equal incubation periods at 34 degrees Celsius. It is important to note that pMJ1 (left) represents a 10^{-1} dilution, while R487I (right) represents a more dilute 10^{-3} dilution, as these dilutions were chosen in order to obtain colony values between the statistically viable value range of 30 - 300.

3D-Structure Analysis

PyMol software was used to observe the 3-dimensional structure of Human Topoisomerase IIα with bound Etoposide (Figure 19a). Template "5gwk" was used to upload topoisomerase into the PyMol database (*RCSB Protein Data Bank* 2016). Mapping each mutated residue showed the proximity of the R487I mutation to the Etoposide binding residues, but also the non-uniform occurrence pattern of mutation location. Figure 19b offers a linearized model of the amino acid sequence with mapped domains, allowing us to designate our 14 discovered mutations to each of the prominent domains in Human Topoisomerase IIα.

a)

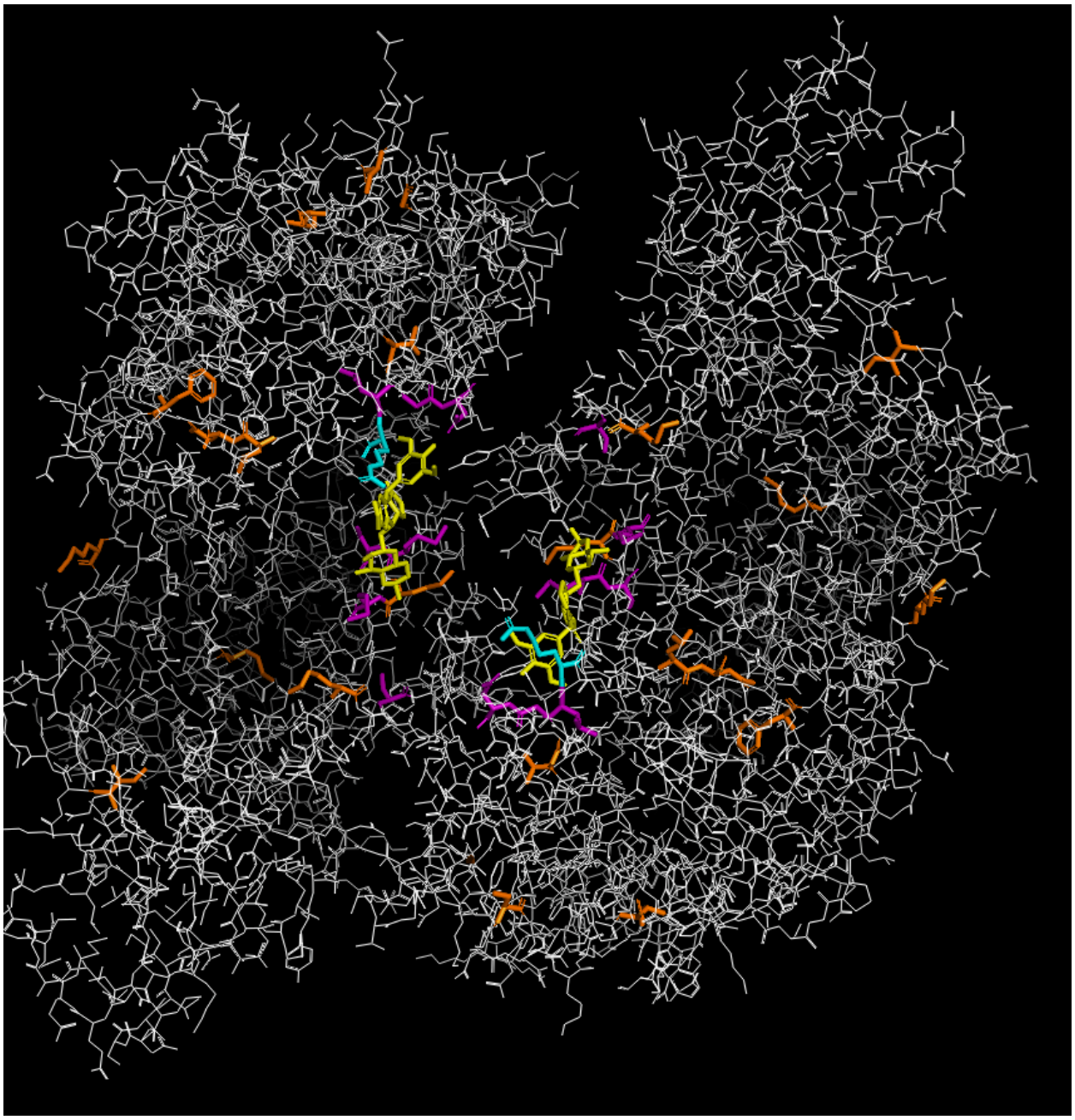

b)

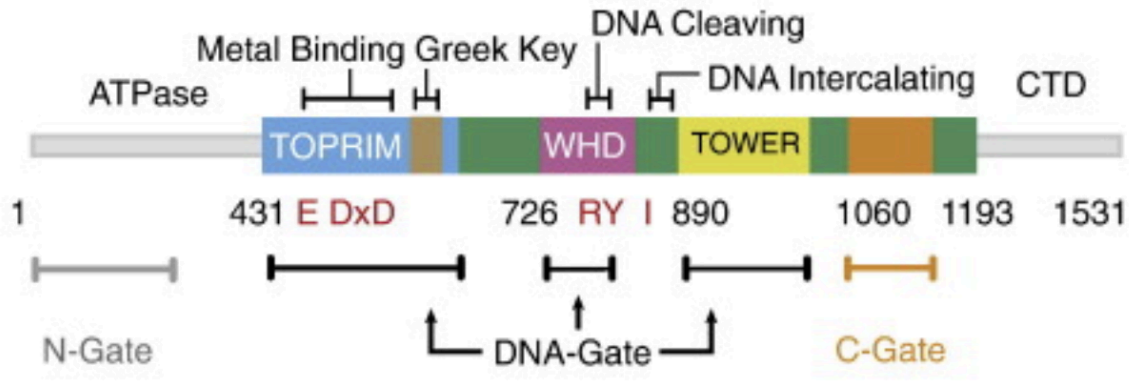

Mutations by Domain:

TOPRIM: XXXXXX
General DNA Binding (Green): XXX
ATPase: X
WHD: XX
TOWER: X

Figure 19 3D-Structure of Human Topoisomerase IIα. a) Residues with highlighted Etoposide (yellow), binding residues (purple), R487I (blue), and 13 non-R487I potent mutants (orange). Source adapted from PyMol Software. b) Mutations localized, assigning each of our 14 discovered potent mutations to one of Human Topoisomerase IIα's catalytic domains. Source adapted from ScienceDirect.

Discussion

Overview of Results

Using a directed-evolution strategy in *Saccharomyces cerevisiae* yeast, we identified multiple hTOP2A amino-acid substitutions that reproducibly reduce sensitivity to Etoposide. In accordance with the ultimate goal of our experiment, we discovered several single substitutions (e.g., R487I, L491F) conferring high-level resistance, allowing researchers to understand common roadblocks to 100% efficacy with Etoposide, and treatment teams to screen cancer patients' genomes before prescribing the drug.

The resistance phenotypes observed in this study were not randomly distributed across the TOP2A sequence. Through the utilization of gap plasmids, our aim was to localize induced mutations throughout the genome, ensuring full representation and observing if potential uniform distribution of mutations conferring resistance was possible. Instead, resistant variants clustered in discrete regions of the protein, especially within and near the TOPRIM-containing cleavage core, suggesting that Etoposide tolerance is shaped by structural constraints rather than by arbitrary sequence change. Although many mutants retained measurable growth at lower drug concentrations, only a subset preserved resistance at 100 μg/mL, indicating that resistance strength varies substantially across mutations rather than producing a simple on/off phenotype. The strongest variant, R487I, is especially notable because it lies in a highly conserved catalytic region and retained robust survival under conditions that eliminated most other mutants. These patterns suggest that the mutations most capable of conferring resistance may act by subtly altering cleavage-complex dynamics while preserving enough catalytic function for cell survival.

As evidenced by the heat map and graphs of relative mutant survival at 30 ng/uL and 100 ng/uL (Figure 16), R487I represents a single nucleotide polymorphism that possesses the

strongest, most robust resistance to Etoposide among each of our 96 unique mutants. The discovery is significant, as R487 was previously implicated in Amsacrine studies as a potential site of topo inhibitor resistance (Sader and Wu 2017). Amsacrine works via the same mechanism as Etoposide (*Liv Hospital* 2026) – stabilizing the cleaved DNA-enzyme intermediate – so R487's position as a binding residue furthers our understanding of its effect on the enzyme-drug interaction.

From an initial pool of sequenced isolates, fourteen mutants demonstrated sustained growth across increasing drug concentrations, with several single-site substitutions conferring particularly robust resistance relative to wild-type. Recurrent mutations at specific residues suggest non-random enrichment and indicate that discrete regions of Topoisomerase IIα play a disproportionate role in mediating drug response. Importantly, resistance was observed across a spectrum of magnitudes, consistent with graded shifts in enzyme-drug interaction rather than binary loss of function. Collectively, these findings expand the current map of residues capable of conferring Etoposide sensitivity and demonstrate the utility of selection-based mutagenesis for uncovering both expected (i.e. mutations found in previous studies with Etoposide and/or with other topo inhibiting drugs) and previously uncharacterized resistance determinants.

Clustering

Mutations within the catalytic domains of an enzyme typically produce deleterious or inactivating phenotypes due to the structural and mechanistic constraints of these regions (Stefl et al. 2013). The fact that all six mutants within the TOPRIM-containing segment retained sufficient catalytic activity to support growth under Etoposide selection indicates that these substitutions do not abolish enzymatic function. Instead, they likely represent finely tuned

alterations that preserve strand passage while selectively destabilizing the drug-stabilized cleavage complex. This balance between maintained catalytic competence and reduced drug susceptibility highlights the functional plasticity of the TOPRIM region and reinforces the idea that resistance arises through subtle modulation of catalytic dynamics rather than loss of activity.

Notably, R450Q -- previously characterized as a multi-drug resistance mutation by Mao and colleagues in 1999 -- also resides within this segment, further underscoring its functional importance (Mao et al. 1999). Because the TOPRIM region contributes to formation of the DNA gate and stabilization of the cleavage complex, and given that Etoposide works by freezing topoisomerase in its DNA-cleavage state prior to religation, mutations within this hotspot are likely to influence interactions among the enzyme, DNA, and drug. Several substitutions in this cluster involve shifts in charge or polarity, suggesting that localized electrostatic or conformational changes may subtly destabilize the drug-trapped cleavage complex. The repeated emergence of independently selected resistance mutations within the TOPRIM-containing portion of the cleavage core therefore supports the hypothesis that resistance arises through targeted modulation of catalytic domain dynamics rather than global disruption of enzyme function.

However, the mutations within the TOPRIM region present an interesting case, as typically mutations to a catalytic region of a gene result in a debilitating, inactivating phenotype. In the case of our six mutations with alterations in this region (G448R, S452Y, T460N, L491F, N492S, R487I), catalytic activity was preserved, even heightened, in order to allow for growth on URA- plates in the presence of Etoposide.

In addition to the 448-492 hotspot, four potent resistance mutations (I765M, M847T, K798N, and I899N) localize within the central region of the DNA cleavage core and reside in

structural proximity to the catalytic tyrosine (Y805) of Topoisomerase IIα. Tyr805 forms the linkage with DNA during double-strand cleavage via nucleophilic attack (Wendorff et al. 2013), representing the catalytic center of the cleavage complex stabilized by Etoposide. The spatial clustering of these mutations around Y805 suggests that resistance may also arise through manipulation of the catalytic environment itself. Several of these substitutions alter residue polarity or charge (e.g., K798N, I899N, M847T), potentially influencing local electrostatics and, in turn, DNA positioning. While direct kinetic measurements would be required to establish causality, their proximity to the catalytic residue supports the hypothesis that resistance may involve subtle destabilization of the drug-trapped cleavage complex rather than disruption of overall enzymatic kinetic parameters. This secondary cluster therefore reinforces the notion that resistance-conferring mutations preferentially localize to structurally and functionally critical regions of the cleavage core.

Among our 14 mutations (I246N, G448R, S452Y, T460N, L491F, N492S, R487I, I636T, F653S, M765I, K798N, M847T, I899N, K1011E), 13 present in the catalytic core, ranging approximately from amino acids 431-1193 (Lindsey Jr. et al. 2014). Proximity to both the highly conserved TOPRIM catalytic region as well as to the catalytic Tyrosine-805 residue provides correlative evidence that mutations affecting DNA's ability to interact with the catalytic regions of topoisomerase also provide some of the most potent resistance against Etoposide. I246N, the only mutation not featured within the catalytic core, resides in a conserved region of the N-terminal. The engine of each of Topoisomerase IIα's functions, ranging from chromosome cohesion, segregation, and condensation, I246N and all other GAP1 mutations display how alterations in the ATPase domain can be equally harmful as it relates to overall enzyme functionality.

R487I's Impact on Topoisomerase IIα Function

Among all identified mutants, R487I emerged as the most striking and significant variant. This substitution conferred greater than 50% resistance even at 100 μg/mL Etoposide, a level at which all other mutants exhibited substantially diminished viability. The magnitude of resistance associated with R487I distinguishes it from the broader mutation set and suggests that residue 487 occupies a particularly influential position in mediating drug sensitivity. Importantly, Arg487 lies firmly within the TOPRIM domain (residues ~450 - 570) of Topoisomerase IIα, a highly conserved catalytic region of the DNA cleavage core responsible for both DNA cleavage and religation. Its localization within this structurally and catalytically critical region underscores the functional weight of this mutation.

The R487I substitution represents a dramatic shift from a positively charged, hydrophilic potentially DNA-interacting arginine to a hydrophobic isoleucine (Figure 20). Within the TOPRIM domain, arginine residues frequently contribute to electrostatic stabilization of the negatively charged phosphodiester backbone of DNA or participate in maintaining the precise geometry of the catalytic site. Loss of positive charge at position 487 may alter local electrostatics or active-site architecture, reducing stabilization of the Etoposide-trapped cleavage complex while preserving sufficient catalytic activity for cell survival. However, a mutation substituting Arg487 with lysine has been shown to confer heightened resistance to Amsacrine (Sader and Wu). Because lysine retains a positive charge, this finding suggests that resistance at this position is not solely dependent on loss of electrostatic interactions. However, based on pKa values, the charge of arginine at physiological pH is still a more strong positive charge than that of lysine, so it is unreasonable to fully rule out electrostatic implications as given that Amsacrine and Etoposide both exert their effect by stabilizing the cleaved DNA-enzyme intermediate, a

mutation that destabilizes this complex without abolishing cleavage activity would provide a strong selective advantage. Therefore, the resistance observed in our R487I mutant is unlikely to arise purely from loss of positive charge and may instead reflect altered structural or steric interactions at this site.

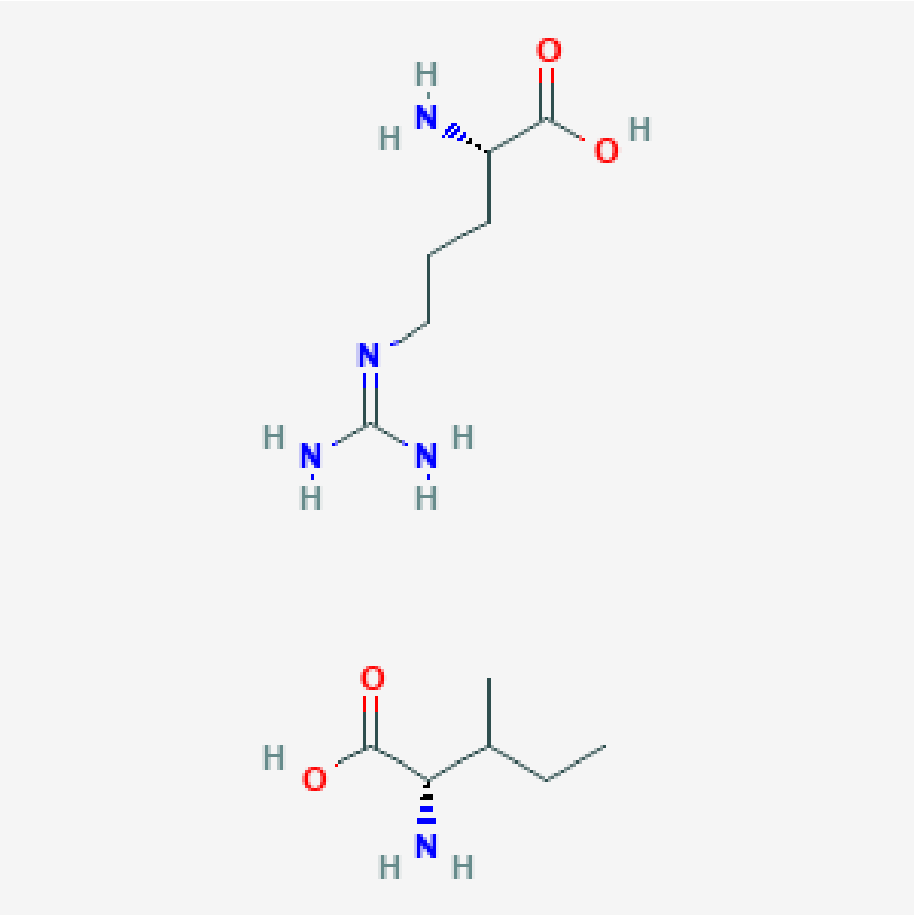

Figure 20 Structures of Arginine and Isoleucine Amino Acids. Arginine (top) and isoleucine (bottom) (National Center for Biotechnology Information 2026).

The exceptional resistance phenotype of R487I, combined with its strategic positioning within the TOPRIM-containing cleavage core, strongly supports the model that Etoposide

resistance in this system arises through targeted modulation of catalytic domain dynamics rather than impairment of enzyme function.

Comparison to Previous Studies

Our discovered mutations in this study offer points of comparison from the previously discovered mutations conferring Etoposide resistance by Hsiung and colleagues in 1996. Characterized mutations R450Q and P803S reside firmly within the established clusters of the TOPRIM region (~450 - 520) and catalytic Tyrosine at position 805. R450Q represents a loss of positive charge in the catalytic domain, believed to weaken the conformational transitions required for the DNA cleavage complex formation. Conversely, P803S represents a transition from the most sterically hindered amino acid in proline to a polar alternative in serine. While R450Q alters local flexibility in the catalytic core, P803S exerts its effect in close proximity to Tyr805. The variants identified in Hsiung and colleagues's study highlighted the pathways by which genetic mutations can affect enzyme function as a whole, focusing on changes in electrostatics, hindrance, and DNA positioning.

The distribution and behavior of resistant mutants observed in this study suggest that Etoposide resistance is driven not simply by the presence of mutations, but by their structural impact on the Topoisomerase IIα cleavage complex. In particular, the strong resistance phenotype observed for R487I, alongside clustering of mutations within the catalytic core, supports the idea that resistance arises from subtle perturbations in drug–enzyme interactions rather than complete disruption of enzymatic function. Because these mutants retain sufficient activity to support growth, the data are most consistent with a mechanism in which mutations

reduce the stability of the drug-stabilized cleavage complex, thereby decreasing the accumulation of cytotoxic double-strand breaks.

This interpretation is further supported by computational work such as Computational analysis of Amsacrine resistance in Human Topoisomerase IIα mutants by Sader and Wu, who examined analogous resistance mutations (R487K and E571K) using homology modeling and molecular dynamics simulations (Sader and Wu 2017). Their findings demonstrated that resistance is associated with a significant reduction in drug binding energy, with the strongest resistance mutation (R487K) showing the greatest impairment. Importantly, their energy decomposition analysis revealed that this weakening primarily arises from disrupted ligand–protein interactions rather than ligand–DNA interactions. This distinction is critical, as it suggests that resistance is mediated by localized structural changes at the drug-binding interface rather than global destabilization of the ternary complex.

Taken together, these computational insights provide a mechanistic framework for interpreting the experimental results presented here. The identification of R487I as the most resistant variant in this study aligns with prior evidence that this residue plays a key role in stabilizing drug binding within the Topoisomerase IIα cleavage complex. While the substitution observed here (isoleucine) differs from the previously characterized lysine mutation, both alterations likely perturb the local interaction network surrounding the drug-binding pocket. This supports a model in which resistance arises from mutation-specific modulation of binding energetics and protein dynamics, reinforcing the broader conclusion that genetic variation within the Topoisomerase IIα catalytic core can preconfigure resistance phenotypes prior to drug exposure.

Pharmacoeconomic Analysis

Small-cell lung cancer (SCLC) is an aggressive malignancy that carries one of the poorest long-term prognosis among all forms of cancers due to its rapid early metastasis rates (Rudin et al. 2021). Etoposide has been used as a first-line therapy for SCLC patients over the past several decades. More specifically, the cornerstone of top-choice therapy for all forms of SCLC has been platinum-Etoposide combination chemotherapy, most commonly cisplatin or carboplatin paired with Etoposide (*Macmillan Cancer Support* 2025). This regimen produces high response rates and remains a standard practice globally due to its simplicity and widespread acceptance by the medical community.

Further analyses, such as a pharmacoeconomic study conducted in India, illustrate the real-world impact of platinum-Etoposide regimens. In that study, a majority of low socioeconomic status patients with metastatic lung cancer received cisplatin-Etoposide as first-line therapy, and the initial six months of treatment demonstrated a statistically significant survival benefit compared with alternative platinum-based doublets (Kamath 2016). Beyond efficacy, the regimen was associated with notable cost-effectiveness, especially in relation to the newer, extremely high-cost cytotoxic agents, reinforcing its role as a frontline therapy in resource-limited settings. These findings underscore that Etoposide remains a mainstay in SCLC therapy globally, particularly where access to newer agents or combination regimens may be restricted. Consequently, understanding the mechanisms by which tumor cells acquire resistance to Etoposide is of direct clinical significance, as failure of this baseline therapy can substantially worsen patient outcomes, both in survival and in quality of life.

Although this study does not perform a formal pharmacoeconomic analysis, our investigation into TOP2A mutations provides a mechanistic basis for the observed variability in

patient responses to Etoposide-containing regimens. By identifying hotspots within the DNA cleavage core, including the highly penetrant R487I mutation, we demonstrate that even within a uniform treatment protocol, intrinsic or acquired genetic differences can drastically alter drug sensitivity. In the context of the cisplatin-Etoposide regimen, these findings suggest that resistance-conferring mutations may explain why certain patients fail to achieve the early tumor shrinkage that is critical for survival advantage in the first six months of therapy. This mechanistic insight adds a molecular dimension to the pharmacoeconomic and clinical observations, highlighting the potential for genotype-guided therapeutic decision-making.

Ultimately, integrating our resistance findings with tried-and-true clinical protocols could improve personalized treatment strategies in SCLC. A 1986 study by Hideki Fukata and colleagues showed a rapid way to isolate Topoisomerase IIα from mammalian cells, through "polyethylene glycol fractionation, ammonium sulfate precipitation, and column chromatography on CM-Sephadex, hydroxyapatite and phosphocellulose" (Fukata et al. 1986). Having an efficient, accepted practice to isolate topoisomerase is critical for the real world application of our experiment's findings. Identification of TOP2A mutations following sequencing of the patient's isolated Topoisomerase IIα could guide clinicians in selecting alternative therapies for patients at risk of Etoposide failure, potentially reducing exposure to ineffective treatment and improving progression-free survival. In resource-limited settings, where platinum-Etoposide remains the standard of care, such predictive insight could maximize the benefit of an already accessible and cost-effective regimen while minimizing wasted cycles of therapy in patients unlikely to respond.

Future Directions

Our study revealed that our discovered mutations to Human Topoisomerase IIα alter enzyme function by weakening Etoposide-DNA cleavage complex stabilization without abolishing enzymatic activity. Because the enzyme retained viability and functionality as evidenced by continuous -- and even improved -- growth, our hypothesis that genetic mutations in the Human Topoisomerase IIα coding region were the basis for resistance against Etoposide was confirmed. However, several avenues for extended investigation could provide further clarity.

First, Michaelis-Menten kinetics could be studied for any of our selected mutants to assess their binding to Etoposide. Measuring parameters such as Vmax and Km for a DNA probe substrate would determine whether our mutations alter catalytic efficiency or substrate affinity relative to wild-type topoisomerase IIα. If catalytic turnover rates (Kcat) remain largely unchanged despite strong resistance phenotypes, this would further support the conclusion that these mutations do not impair topoisomerase IIα function but instead reduce the ability of Etoposide to stabilize the cleavage complex. Similarly, for mutations located within or near the ATPase domain, assessing ATP hydrolysis kinetics could reveal whether altered energy coupling contributes to resistance. Together, such kinetic studies would help distinguish between changes in baseline catalytic activity and drug-specific modulation of cleavage complex dynamics.

Further, an important next step would be to validate these resistance-conferring mutations in a mammalian cell system. Although the directed evolution screen was performed in yeast, Human Topoisomerase IIα functions within a more complex environment in cancer cells. Introducing selected mutations, such as R487I, into mammalian cell lines using CRISPR-based genome editing or expression constructs (obtained from GeneWiz) would determine whether the

resistance phenotypes observed in yeast translate to human cellular contexts. Measuring cell viability following Etoposide treatment would clarify the clinical relevance of these substitutions. This line of testing would strengthen the connection between our mechanistic findings and potential therapeutic resistance in human tumors.

Unlike yeast, mammalian cells possess additional layers of DNA damage surveillance, including the TP53 pathway (Chen 2016). In response to Etoposide-induced double-strand breaks, p53 activates transcriptional programs that promote apoptosis (via BAX, BAD, and PUMA) or cell cycle arrest via p21 (Chen 2016). Introducing resistance-conferring TOP2A mutations into mammalian cells would allow us to assess whether these variants decrease DNA damage signaling and reduce p53 activation following Etoposide treatment by assessing the presence and activity of these proteins via immunoprecipitation experiments or Western blotting. Such experiments would clarify whether resistance not only preserves topoisomerase function but also dampens downstream anti-cancer responses.

Work from earlier comparative studies also supports the idea that testing mutations in mammalian cell lines could provide valuable insight. Vassetzky in 1995 showed that Topoisomerase IIα mutations linked to drug resistance tend to affect similar regions of the enzyme in a variety of tumor lines. The study utilized drug-resistant cells from human patients, animal cells, and “simple” yeast cells, finding that the resulting resistance phenotype to Etoposide (and amsacrine) is often a direct result of either mutations in topoisomerase IIα’s catalytic sites, or enhanced expression of the *MDR* gene family (Vassetzky 1995). Using multiple systems to test strong variants like R487I or S452Y would therefore help us determine whether the effects we see in yeast reflect how these mutations behave in human cells. Further, the

differences in model systems would allow us to observe if these mutations influence downstream variables like DNA-damage responses.

Another informative direction would be to analyze double mutants in order to determine whether resistance effects are additive, synergistic, or antagonistic. Combining two resistance-conferring substitutions could reveal whether their effects accumulate to produce greater drug tolerance, or whether one mutation dominates the phenotype. For example, introducing a second mutation alongside a potent mutation like R487I would help determine whether resistance is further enhanced by the introduction of, for example, K1011E. Conversely, certain substitutions may partially suppress or counteract the resistance phenotype of a stronger mutation, revealing functional interactions between residues within the catalytic core. We can begin exploring these relationships by revisiting and deconvoluting the double mutants that were initially identified during sequencing but excluded from advancement to primary screening. Phenotypic assays of these combinations would provide insight into residue-by-residue interactions within topoisomerase IIα and clarify whether resistance arises through independent additive effects or coordinated efforts to destabilize the drug-enzyme-DNA complex.

Moreover, further three-dimensional structural analysis using PyMOL is a logical next step in linking our identified mutations to changes in protein structure. By mapping each substitution onto the structure of topoisomerase IIα, we can measure the distance between mutated residues and known Etoposide-binding sites, both before and after substitution. This approach would clarify whether resistance arises from direct proximity effects, altered electrostatics, or steric interference within the drug-binding pocket. Although our study identified primary sequence alterations with clear functional consequences, their impact on tertiary and quaternary structure remains undefined.

Conclusion

Our findings broaden the current understanding of how single-site alterations within Human Topoisomerase IIα influence Etoposide response. By integrating random mutagenesis with functional selection through our directed evolution experiment, this study reveals that resistance can arise from diverse structural regions of the enzyme, including residues not directly involved in drug binding. However, disproportionate concentrations within the TOPRIM region and surrounding the Tyrosine-805 catalytic outline hotspots for genetic mutations that possess capabilities to confer resistance to powerful chemotherapeutic agent Etoposide. More broadly, this work highlights the value of directed evolution approaches in anticipating clinically relevant resistance pathways and provides a framework for future efforts aimed at refining chemotherapeutic design and guiding more individualized treatment strategies that improve patient outlooks.

References

Acuna-Hidalgo, R., Veltman, J. A., & Hoischen, A. (2016). New insights into the generation and role of de novo mutations in health and disease. Genome Biology, 17(1), 241. https://doi.org/10.1186/s13059-016-1110-1

Agilent Technologies, Inc. (2015). QuikChange HT protein engineering system protocol (Publication No. G5900-90000, Version B.0). https://www.agilent.com/library/usermanuals/Public/G5900-90000.pdf

Allinen, M., Beroukhim, R., Cai, L., Brennan, C., Lahti-Domenici, J., Huang, H., Porter, D., Hu, M., Chin, L., Richardson, A., Schnitt, S., Sellers, W. R., & Polyak, K. (2004). Molecular characterization of the tumor microenvironment in breast cancer. Cancer Cell, 6(1), 17–32. https://doi.org/10.1016/j.ccr.2004.06.010

American Cancer Society. (2020, November 6). Signs and symptoms of cancer. https://www.cancer.org/cancer/diagnosis-staging/signs-and-symptoms-of-cancer.html

American Cancer Society. (2022, August 31). Oncogenes, Tumor Suppressor Genes, and DNA Repair Genes. Www.cancer.org; American Cancer Society. https://www.cancer.org/cancer/understanding-cancer/genes-and-cancer/oncogenes-tumor-suppressor-genes.html

Lizano Soberón, M., & Barrera Rodríquez, R. (1993). Resistencia múltiple a drogas: un problema en la quimioterapia de cáncer [Multiple drug resistance: a problem in cancer chemotherapy]. Revista de investigacion clinica; organo del Hospital de Enfermedades de la Nutricion, 45(5), 481–492.

Bates, S. (2025). Deoxyribonucleic acid (DNA). Genome. https://www.genome.gov/genetics-glossary/Deoxyribonucleic-Acid-DNA

Biomiga, Inc. (n.d.). EZgene™ DNA/RNA/protein isolation kit (Catalog No. DR3211) user manual. https://biomiga.com/wp-content/uploads/2021/09/DR3211-DNA.RNA_.Protein-Isolation-Kit.pdf

Brink, M., Meeuwes, F. O., van der Poel, M. W. M., Kersten, M. J., Wondergem, M., Mutsaers, P. G. N. J., Böhmer, L. H., Woei-A-Jin, F. J. S. H., Visser, O., Oostvogels, R., Jansen, P. M., Plattel, W., Huls, G. A., Vermaat, J. S. P., & Nijland, M. (2022). Impact of etoposide and ASCT on survival among patients aged <65 years with stage II to IV PTCL: A population-based cohort study. Blood, 140(9), 1009–1019. https://doi.org/10.1182/blood.2021015114

Chen, J. (2016). The cell-cycle arrest and apoptotic functions of p53 in tumor initiation and progression. Cold Spring Harbor Perspectives in Medicine, 6(3), a026104. https://doi.org/10.1101/cshperspect.a026104

Cowell, I. G., Sondka, Z., Smith, K., Lee, K. C., Manville, C. M., Sidorczuk‐Lesthuruge, M., Rance, H. A., Padget, K., Jackson, G. H., Adachi, N., Austin, C. A., & Alghisi, G. (2018). Model for MLL translocations in therapy‐related leukemia involving topoisomerase IIβ‐mediated DNA strand breaks and gene proximity. Nature Communications, 9, 1. https://doi.org/10.1038/s41467-018-05406-y

Cuya, S. M., Bjornsti, M. A., & van Waardenburg, R. C. A. M. (2017). DNA topoisomerase-targeting chemotherapeutics: What's new? Cancer Chemotherapy and Pharmacology, 80(1), 1–14. https://doi.org/10.1007/s00280-017-3334-5

D'Arpa, P., Beardmore, C., & Liu, L. F. (1990). Involvement of nucleic acid synthesis in cell killing mechanisms of topoisomerase poisons. Cancer Research, 50(21), 6919–6924.

Dean M. The Human ATP-Binding Cassette (ABC) Transporter Superfamily. Bethesda (MD): National Center for Biotechnology Information (US); 2002 Nov 18. Available from: https://www.ncbi.nlm.nih.gov/books/NBK3/

Elshafei, A., Al-Toubat, M., Feibus, A. H., Koul, K., Jazayeri, S. B., Lelani, N., Henry, V., & Balaji, K. C. (2023). Genetic mutations in smoking-associated prostate cancer. The Prostate, 83(13), 1229–1237. https://doi.org/10.1002/pros.24554

Etoposide and cisplatin chemotherapy (EP). (2025). Macmillan Cancer Support. https://www.macmillan.org.uk/cancer-information-and-support/treatments-and-drugs/Etoposide-and-cisplatin-ep

Farsani, F. M., & Sadeq, V. (2018). Variations related to resistance of cancer cells to topoisomerase II alpha inhibitory drugs. Bioinformatics & Proteomics Open Access Journal, 2(1), 000122. https://medwinpublishers.com/BPOJ/BPOJ16000122.pdf

Fukata, H., Ohgami, K., & Fukasawa, H. (1986). Isolation and characterization of DNA topoisomerase II from cauliflower inflorescences. Plant Molecular Biology, 6(3), 137–144. https://doi.org/10.1007/BF00021482

Ganapathi, R. N., & Ganapathi, M. K. (2013). Mechanisms regulating resistance to inhibitors of topoisomeraseII. Frontiers in Pharmacology, 4, 89. https://doi.org/10.3389/fphar.2013.00089

Global Cancer Facts & Figures. (2024). Www.cancer.org. https://www.cancer.org/research/cancer-facts-statistics/global-cancer-facts-and-ss.html

Guan, Y., Yao, Q., Hao, Y., Zeng, X., Wang, W., Gu, X., Xiang, J., Sun, Y., & Song, Z. (2023). The combination of etoposide and platinum for the treatment of thymic neuroendocrine neoplasms: A retrospective analysis. Cancer Medicine, 12(15), 16011–16018. https://doi.org/10.1002/cam4.6245

Hande, K. R. (1998). Etoposide: Four decades of development of a topoisomerase II inhibitor. European Journal of Cancer, 34(10), 1514–1521. https://doi.org/10.1016/S0959-8049(98)00228-7 (doi.org in Bing)

Hsiung, Y., Jannatipour, M., Rose, A., McMahon, J., Duncan, D., & Nitiss, J. L. (1996). Functional expression of Human Topoisomerase IIα in yeast: Mutations at amino acids 450 or 803 result in enzymes that confer resistance to anti-topoisomerase II agents. Cancer Research, 56(1), 91–99.

Jaffrézou, J. P., Chen, K. G., Durán, G. E., Kühl, J. S., & Sikic, B. I. (1994). Mutation rates and mechanisms of resistance to etoposide determined from fluctuation analysis. Journal of the National Cancer Institute, 86(15), 1152–1158. https://doi.org/10.1093/jnci/86.15.1152

Johnson, D. H., Hainsworth, J. D., Hande, K. R., & Greco, F. A. (1991). Current status of etoposide in the management of small cell lung cancer. Cancer, 67(1 Suppl), 231–244. https://doi.org/10.1002/1097-0142(19910101)67:1+

Kamath, M. P., Lakshmaiah, K. C., Babu, K. G., Loknatha, D., Jacob, L. A., & Babu, S. M. (2016). Pharmacoeconomic benefit of cisplatin and etoposide chemoregimen for metastatic non–small cell lung cancer: An Indian study. Lung India, 33(2), 154–158. https://doi.org/10.4103/0970-2113.177448

Lee, J. H., & Berger, J. M. (2019). Cell cycle–dependent control and roles of DNA topoisomerase II. Genes, 10(11), 859. https://doi.org/10.3390/genes10110859

Lichtenstein, A. V. (2010). Cancer: Evolutionary, genetic and epigenetic aspects. Clinical Epigenetics, 1(3–4), 85–100. https://doi.org/10.1007/s13148-010-0010-6

Lindsey, R. H., Jr., Pendleton, M., Ashley, R. E., Mercer, S. L., Deweese, J. E., & Osheroff, N. (2014). Catalytic core of Human Topoisomerase IIα: Insights into enzyme–DNA interactions and drug mechanism. Biochemistry, 53(41), 6595–6602. https://doi.org/10.1021/bi5010816

Liv Hospital. (2026). Amsacrine. Liv Hospital. https://int.livhospital.com/drugs/amsacrine/

Mak, C. K., Hung, V. K., & Wong, J. T. (2005). Type II topoisomerase activities in both the G1 and G2/M phases of the dinoflagellate cell cycle. Chromosoma, 114(6), 420–431. https://doi.org/10.1007/s00412-005-0027-3

Mao, Y., Yu, C., Hsieh, T. S., Nitiss, J. L., Liu, A. A., Wang, H., & Liu, L. F. (1999). Mutations of Human Topoisomerase II alpha affecting multidrug resistance and sensitivity. Biochemistry, 38(33), 10793–10800. https://doi.org/10.1021/bi9909804

McIntosh, S. A., Alam, F., Adams, L., Boon, I. S., Callaghan, J., Conti, I., Copson, E., Carson, V., Davidson, M., Fitzgerald, H., Gautam, A., Jones, C. M., Kargbo, S., Gokul Lakshmipathy, Maguire, H., McFerran, K., Amatta Mirandari, Moore, N., Moore, R., & Murray, A. (2023). Global funding for cancer research between 2016 and 2020: a content analysis of public and philanthropic investments. The Lancet Oncology, 24(6), 636–645. https://doi.org/10.1016/s1470-2045(23)00182-1

Mollaei, M., Hassan, Z. M., Khorshidi, F., & Langroudi, L. (2021). Chemotherapeutic drugs: Cell death- and resistance-related signaling pathways. Translational Oncology, 14(5), 101056. https://doi.org/10.1016/j.tranon.2021.101056

Montecucco, A., Zanetta, F., & Biamonti, G. (2015). Molecular mechanisms of etoposide. EXCLI Journal, 14, 95–108. https://doi.org/10.17179/excli2015-561

National Cancer Institute. (2025, May 7). Cancer Statistics. National Cancer Institute. https://www.cancer.gov/about-cancer/understanding/statistics

National Cancer Institute. (2019, May 16). Symptoms. National Cancer Institute; Cancer.gov. https://www.cancer.gov/about-cancer/diagnosis-staging/symptoms

National Center for Biotechnology Information. (2024). Etoposide: PubChem compound summary. https://pubchem.ncbi.nlm.nih.gov/compound/Etoposide

National Research Council (US) Committee on Mapping and Sequencing the Human Genome. (2016). Introduction. National Academies Press. https://www.ncbi.nlm.nih.gov/books/NBK218247/

NCI Dictionary of Cancer Terms. (2026). Cancer.gov. https://www.cancer.gov/publications/dictionaries/cancer-terms/def/drug-resistance.

New England Biolabs. (2021). Monarch® PCR & DNA cleanup kit (5 µg) instruction manual (Version 3.0). https://www.neb.com/en-us/-/media/nebus/files/manuals/manualt1030.pdf

Nielsen, C. F., Zhang, T., Barisic, M., Kalitsis, P., & Hudson, D. F. (2020). Topoisomerase IIα is essential for maintenance of mitotic chromosome structure. Proceedings of the National Academy of Sciences, 117(22), 12131–12142. https://doi.org/10.1073/pnas.2001760117

Nitiss, J. L. (2009). DNA topoisomerase II and its growing repertoire of biological functions. Nature Reviews Cancer, 9(5), 327–337. https://doi.org/10.1038/nrc2608

Nitiss, J. L. (2013). Targeting DNA topoisomerase II in cancer chemotherapy. Nature Reviews Cancer, 13(5), 338–351. https://doi.org/10.1038/nrc3490

Patel, M. M., & Adrada, B. E. (2024). Hereditary breast cancer: BRCA mutations and beyond. Radiologic Clinics of North America, 62(4), 627–642. https://doi.org/10.1016/j.rcl.2023.12.014

Perez-Soler, R., Glisson, B. S., Lee, J. S., Fossella, F. V., Murphy, W. K., Shin, D. M., & Hong, W. K. (1996). Treatment of patients with small-cell lung cancer refractory to etoposide

and cisplatin with the topoisomerase I poison topotecan. Journal of Clinical Oncology, 14(10), 2785–2790. https://doi.org/10.1200/JCO.1996.14.10.2785

Pfeifer G. P. (2020). Mechanisms of UV-induced mutations and skin cancer. Genome instability & disease, 1(3), 99–113. https://doi.org/10.1007/s42764-020-00009-8

Pommier, Y., Leteurtre, F., Fesen, M. R., Fujimori, A., Bertrand, R., Solary, E., Kohlhagen, G., & Kohn, K. W. (1999). Cellular determinants of sensitivity and resistance to DNA topoisomerase inhibitors. Cancer Investigation, 17(6), 572–584. https://doi.org/10.3109/07357909909032875

RCSB Protein Data Bank (2016). 5GWK: Human topoisomerase IIalpha in complex with DNA and etoposide. Rcsb.org. https://www.rcsb.org/structure/5GWK

Rima. (2020, December 23). Pharmacology of etoposide. BioPharma Notes. https://biopharmanotes.com/pharmacology-of-Etoposide/

Rudin, C. M., Brambilla, E., Faivre-Finn, C., & Sage, J. (2021). Small-cell lung cancer. Nature reviews. Disease primers, 7(1), 3. https://doi.org/10.1038/s41572-020-00235-0

Sader, S., & Wu, C. (2017). Computational analysis of Amsacrine resistance in human topoisomerase II alpha mutants (R487K and E571K) using homology modeling, docking and all-atom molecular dynamics simulation in explicit solvent. Journal of Molecular Graphics and Modelling, 72, 209–219. https://doi.org/10.1016/j.jmgm.2016.11.019

Schmutz, A., Salignat, C., Plotkina, D., Devouassoux, A., Lee, T., Arnold, M., Ervik, M., & Kelm, O. (2019). Mapping the global cancer research funding landscape. JNCI Cancer Spectrum, 3(4), pkz069. https://doi.org/10.1093/jncics/pkz069

Siegel, R. L., Giaquinto, A. N., & Jemal, A. (2024). Cancer statistics, 2024. CA: A Cancer Journal for Clinicians, 74(1), 12–49. https://doi.org/10.3322/caac.21820

Sousa, G., de Almeida, M. C. F., Lócio, L. L., Dos Santos, V. L., Bezerra, D. P., Silva, V. R., de Almeida, S. M. V., Simon, A., Honório, T. D. S., Cabral, L. M., Castro, R. N., de Moura, R. O., & Kümmerle, A. E. (2022). Synthesis and Evaluation of Antiproliferative Activity, Topoisomerase IIα Inhibition, DNA Binding and Non-Clinical Toxicity of New Acridine-Thiosemicarbazone Derivatives. Pharmaceuticals (Basel, Switzerland), 15(9), 1098. https://doi.org/10.3390/ph15091098

Stefl, S., Nishi, H., Petukh, M., Panchenko, A. R., & Alexov, E. (2013). Molecular mechanisms of disease-causing missense mutations. Journal of molecular biology, 425(21), 3919–3936. https://doi.org/10.1016/j.jmb.2013.07.014

Swedan, H. K., Kassab, A. E., Gedawy, E. M., & Elmeligie, S. E. (2023). Topoisomerase II inhibitors design: Early studies and new perspectives. Bioorganic Chemistry, 136, 106548. https://doi.org/10.1016/j.bioorg.2023.106548 (doi.org in Bing)

Thorn, C. F., Oshiro, C., Marsh, S., Hernandez-Boussard, T., McLeod, H., Klein, T. E., & Altman, R. B. (2011). Doxorubicin pathways: pharmacodynamics and adverse effects. Pharmacogenetics and genomics, 21(7), 440–446. https://doi.org/10.1097/FPC.0b013e32833ffb56

UniProt Consortium. (2024). TOP2A variant: VAR_007533. https://web.expasy.org/variant_pages/VAR_007533.html

Vanden Broeck, A., Lotz, C., Drillien, R., Haas, L., Bedez, C., & Lamour, V. (2021). Structural basis for allosteric regulation of Human Topoisomerase IIα. Nature Communications, 12, 2962. https://doi.org/10.1038/s41467-021-23136-6

Vassetzky, Y. (1995). DNA topoisomerase II mutations and resistance to anti-tumor drugs. BioEssays, 17(9), 761–770. https://doi.org/10.1002/bies.950170906

Wang, J. C. (1999). Cellular roles of DNA topoisomerases: A molecular perspective. Nature Reviews Molecular Cell Biology, 1(1), 1–11.

Warburton, P. E., & Earnshaw, W. C. (1997). Untangling the role of DNA topoisomerase II in mitotic chromosome structure and function. BioEssays, 19(2), 97–99. https://doi.org/10.1002/bies.950190203

Wendorff, T. J., Schmidt, B. H., Heslop, P., Austin, C. A., & Berger, J. M. (2012). The structure of DNA-bound Human Topoisomerase IIα: Conformational mechanisms for coordinating inter-subunit interactions with DNA cleavage. Journal of Molecular Biology, 424(3–4), 109–124. https://doi.org/10.1016/j.jmb.2012.07.014

Whalen, K., Feild, C., & Radhakrishnan, R. (2019). Lippincott illustrated reviews: Pharmacology (7th ed.). Wolters Kluwer.

Winstead, E. (2022, January 20). How mRNA vaccines might help treat cancer. National Cancer Institute.

https://www.cancer.gov/news-events/cancer-currents-blog/2022/mrna-vaccines-to-treat-cancer

World Health Organization. (2024). Global cancer burden growing, amidst mounting need for services. https://www.who.int/news/item/01-02-2024-global-cancer-burden-growing--amidst-mounting-need-for-services

Xu, X., Zhou, Y., Feng, X., Li, X., Asad, M., Li, D., Liao, B., Li, J., Cui, Q., & Wang, E. (2020). Germline genomic patterns are associated with cancer risk, oncogenic pathways, and clinical outcomes. Science advances, 6(48), eaba4905. https://doi.org/10.1126/sciadv.aba4905

Yeast transformation protocol. (n.d.). https://singerlab.ucdavis.edu/wp-content/uploads/2020/01/YeastTransformation.pdf

Appendix

Appendix A Primers for Mutagenesis PCR, Amplification PCR, and Sequencing PCR

a) Primers for Error-Prone PCR

Primer Name	Mutated Region	Forward or Reverse	Sequence (5'- 3')	Base Pairs Covered (bp)
Alpha 18	Gap 1	Forward	TTACTGTGGAAACAGCCAGTAGA	671
Alpha 1200R	Gap 1	Reverse	TTTGATAAATTTTTCACTCAATTGGCATG	671
Alpha 1001	Gap 2	Forward	TGACTAAACTTGTTGATGTTGTGAAG	714
Alpha 15	Gap 2	Reverse	CCTCCAGAAAACGATGTCGCAG	714
Alpha 25	Gap 3	Forward	AGGTGTCTTCTCGGTGCCA	1217
Alpha 10	Gap 3	Reverse	GTTCCCACATCAAAGGCTTGC	1217
Alpha 7	Gap 4	Forward	GTGCTGAAGGAATCGGTACT	1036

			G	
Alpha 23	Gap 4	Reverse	CCTTTCCCAGGAAGTCCGA	1036

b) Primers for Amplification / Extraction out of Yeast

Primer Name	Amplified Region	Associated Primer	Sequence (5'-3')	Base Pairs Covered (bp)
Alpha 17	Gap 1	Forward	GAGATTCTAGTTAATGCTGCGG	1457
Alpha 15	Gap 1	Reverse	CCTCCAGAAAACGATGTCGCAG	1457
Alpha 18	Gap 2	Forward	TTACTGTGGAAACAGCCAGTAGA	1337
Alpha 14	Gap 2	Reverse	CTTTGATGTGCTGGTGCCC	1337
Alpha 31	Gap 3	Forward	GTGGGTCTTCAGTACAAGAAAAACTATG	1589

Alpha 9	Gap 3	Reverse	GCACCAAGCATTCCTAGGAG	1589
Alpha 6	Gap 4	Forward	CAAACGGAATGACAAGCGAG	1657
AS-2	Gap 4	Reverse	TTTGATTGGCTTAAATGCCAATGTAGT	1657

c) Primers for Sequencing

Primer Name	Sequenced Region	Associated Primer	Sequence (5'- 3')	Base Pairs Covered (bp)
Alpha-18	Gap 1	Forward	TTACTGTGGAAACAGCCAGTAGA	910
Alpha-16	Gap 1	Reverse	TTGTCTCTCCCAACCACACC	910
Alpha-2	Gap 2	Forward	GTGAAGTTTAAGGCCCAAGTCCAG	268
Alpha-1200R	Gap 2	Reverse	TTTGATAAATTTTTCACTCCATTGGCATG	268
Alpha-6	Gap 3	Forward	CAAACGGAATGACAAGCGA	247

			G	
Alpha-12	Gap 3	Reverse	GCTCAGCTCTTTGGCTCGAT TG	247
Alpha-7	Gap 4	Forward	GTGCTGAAGGAATCGGTACT G	238
Alpha-11	Gap 4	Reverse	GAGCTTCCCGTCAGAACATG	238

Appendix B List of All Discovered Mutations

Strain	Description	# Tubes	Location		Strain	Description	# Tubes	Location		Strain	Description	# Tubes	Location				
Box 1					Box 2					Box 3				Box 4			
G9	gap2 A469T, Q500H	2	A1-2		gap 3.30		2	A1-2		Gap4.2	G1007D	2	A1-2	gap2 I47	N560K	2	A1-2
F5	gap2 A465S	2	A3-4		Gap 3.31		2	A3-4		Gap4.5	C862Y,M881I,N945I	2	A3-4	gap 2 A14	no change	2	A3-4
G26	gap2 G404D	2	A5-6		Gap 3.32		2	A5-6		Gap4.6	K1011E	2	A5-6	gap 2 A16	P385A, M537V	2	A5-6
I47	gap2 N560K	2	A7-8		Gap 3.33		2	A7-8		Gap4.7	G1007D	2	A7-8	gap 2 Clone	S452Y	2	A7-8
clone14	gap2 P385S, R494Q	2	A9-10		Gap 3.34		2	B1-2		Gap 4.12	K949M	2	B1-2	gap 2.202	G448W	2	A9-10
F39	gap2 L491I	2	B1-2		Gap 3.35		2	B3-4		Gap4.13	L1144F	2	B3-4	gap 2.203	R487I	2	B1-2
A11	gap2 K550Q	2	B3-4		Gap 3.36		2	B5-6		Gap4.14	L1144F	2	B5-6	gap 2.204	I510T	2	B3-4
H50	gap2 S452Y	2	B5-6		Gap 3.37		2	B7-8		Gap4.16	K1011E	2	B7-8	gap 2.206	G448W	2	B5-6
clone18	gap2 K535M	2	B7-8		Gap 3.38		2	B9-10		Gap 4.101	M943V	2	C1-2	gap 2.207	I403F	2	B7-8
A14	gap2 no change	2	B9-10		Gap 3.39		2	C1-2		Gap4.102	W1036C, A1052V	2	G1-2	gap 2.208	Q422R	2	B9-10
clone13	gap2 N492S, V514M	2	C1-2		Gap 3.40		2	C3-4		Gap4.103	V928I, H986Y,S1117T	2	C3-4	gap 2.209	G448W	2	C1-2
A16	gap2 P385A, M536V	2	C3-4		Gap2.113	V514L, V422F	2	D7-8		Gap4.104	V1015M	2	C5-6	gap 2.210	A419G	2	C3-4
clone15	gap2 R494G	2	C5-6		Gap2.114	A447V	2	E1-2		Gap4.105	no change K1283S	2	C8-9	gap 2.211	I246N, F271I, N537V	2	C5-6
Clone16	gap 2 S452Y	2	c7-8		Gap2.128	T460N	2	E3-4		Gap4.106	L1009F, L1041F	2	D1-2	gap 2.212	S452Y	2	C7-8
Clone17	gap2 G448R	2	c9-10		Gap2.131	N492S	2	E5-6		Gap4.107	I899N mixed	2	F9-10	gap 2.213	G448W	2	C9-10
Clone19	gap2 L491F	2	D1-2		Gap2.134	R450L	2	E7-8		Gap4.108	I899N partial	2	D3-4	gap 2.214	R487I	2	D1-2
Clone20	GAP2 I407M	2	D3-4		Gap2.139	R450L	2	E9-10		Gap4.109	C862F,F867C,R1053H,V1076F,A1093E	2	F6-7	gap 2.215	I510T	2	D3-4
gap3.1	gap3 P682S, F589S,K893M	2	D5-6		Gap2.140	N492S, V514M	2	F1-2		Gap4.110	M1000L	2	D6-7	gap 2.216	G448R	2	D5-6
gap3.2	Q726H, S650N	2	D7-8		Gap2.141	S410G, T456M	2	F3-4		Gap4.111	L991F partial	2	F3-4	gap3.5R	I699F,N894K	2	D7-8
gap3.3	T691I, T694I, L783P	2	D9-10		Gap2.201	M537V	4	D1-2, F5-6		Gap4.112	I494T, N1126I	2	F1-2	gap3.7R	I699F,N894K	2	D9-10
gap3.4	Q726P, K906N, D831E	2	E1-2		Gap2.202	G448W	4	D3-4, F9-10		Gap4.113	F886H,F1163S	2	E9-10	gap3.15	H634F, R672G	2	E1-2
GAP3.5	mixed	2	e3-4		Gap2.203	R487I	4	D5-6, G1-2		Gap4.114	F1023L	2	E6-7	gap3.17	I636T	2	E3-4
GAP3.6	poor seq	2	e5-6		Gap2.204	I510T	2	G3-4		Gap.115	K1011E	2	E3-4	gap3.19	Q906L	2	E5-6
GAP3.7	mixed	2	E7-8		Gap2.205	F556S	2	G5-6		Gap4.116	K1011E	2	E1-2	gap3.21	F653S	2	E7-8
gap3.8	Y686F	2	E9-10		Gap2.206	G448W	2	G9-10		Gap4.117	K990I,D1120E	2	D9-10	gap3.24	I864F, K936R	2	E9-10
gap3.9	E572V	2	f1-2		Gap2.207	I403F	2	H1-2		Gap4.118	Y935F,G945D,M999I,K1141E	2	G3-4	gap3.28	S891C, E941G	2	F1-2
gap3.10	mixed	2	F3-4		Gap2.208	Q422R	2	H3-4		Gap1.01	G283V	2	G6-7	gap3.29	I658K	2	F3-4
gap3.11	N894Y	2	F5-6		Gap2.209	G448W	2	H7-8		Gap1.02	R450Q	2	G9-10	gap3.30	D710G	2	F5-6
gap3.12	G777D	2	F7-8		gap2.210	A419G	2	H9-10		Gap1.04	V228A, G322S	2	H1-2	gap3.31	N780I, F573Y	2	F7-8
gap3.13	L665S	2	F9-10		Gap2.211	I246N,F271I,N537V	2	I1-2		Gap1.05	K342M	2	H3-4	gap3.32	Q863R, K739R, I864F	2	F9-10
gap3.14	H759N, F867Y	2	G1-2		Gap2.212	S452Y	2	I3-4		Gap1.06	T372I	2	H6-7	gap3.33	M847T, F653C	2	G1-2
gap3.15	poor seq	2	G3-4		Gap2.213	G448W	2	I5-6		Gap1.07	I246N	2	H9-10	gap3.34	L889M, R870C	2	G3-4
gap3.16	M765I	2	G7-8		Gap2.214	R487I	2	I9-10		Gap1.09	K342M, Q292E	2	I1-2	gap3.35	N700K	2	G5-6
gap3.17	no seq	2	G9-10		Gap2.215	I510T	2	J1-2		Gap1.12	G348D	2	I3-4	gap3.36	F638I, N667I	2	G7, I1
gap3.18	mixed	2	H1-2		Gap2.216	G448R	2	J5-6		Gap1.18	G283V	2	I6-7	gap3.37	N945D	2	I2-3
gap3.19	Q906L needs confirmation	2	H3-4		Gap2.217	A429T,D526E,K550E	2	J7-8		Gap1.20	V228A, G322S	2	I9-10	gap3.38	F569L, L677F, K821N, T919S	2	I4-5
Gap3.20	F595V, V744I mixed	2	h5-6		Gap2,218	R494G	2	J9-10		Gap1.21	K342M	2	J1-2	gap3.39	P820R, F638Y	2	I6-7
GAP3.21	only F read, no changes	2	h9-10		Gap2.219	T460N	2	J3, I7		Gap1.22	T372I	2	J3-4	gap3.40	E702V	2	I8-9
Gap 3.22	mixed	2	I1-2		Gap3.10R		2	C9-C10		Gap1.23	I246N	2	j5-6				
Gap 3.23	D823V	2	I3-4		Gap3.5R		2	C5-C6		Gap1.25	K342M, Q292E	2	J7-8				
Gap 3.24	poor seq	2	I5-6		Gap3.7R		2	C7-C8		Gap1.28	G348D	2	J9-10				
Gap 3.25	M847T	2	I9-10														
Gap 3.26	F653C	2	J1-2														
Gap 3.27	H759R	2	J3-4														
Gap 3.28		2	J5-6														
Gap 3.29		2	J9-10														

Appendix C Full pMJ1 Sequence

ATGGAAGTGTCACCATTGCAGCCTGTAAATGAAAATATGCAAGTCAACAAAATAAAG

AAAAATGAAGATGCTAAGAAAAGACTGTCTGTTGAAAGAATCTATCAAAAGAAAAC

ACAATTGGAACATATTTTGCTCCGCCCAGACACCTACATTGGTTCTGTGGAATTAGTG

ACCCAGCAAATGTGGGTTTACGATGAAGATGTTGGCATTAACTATAGGGAAGTCACTT

TTGTTCCTGGTTTGTACAAAATCTTTGATGAGATTCTAGTTAATGCTGCGGACAACAA

ACAAAGGGACCCAAAAATGTCTTGTATTAGAGTCACAATTGATCCGGAAAACAATTTA

ATTAGTATATGGAATAATGGAAAAGGTATTCCTGTTGTTGAACACAAAGTTGAAAAGA

TGTATGTCCCAGCTCTCATATTTGGACAGCTCCTAACTTCTAGTAACTATGATGATGAT

GAAAAGAAAGTGACAGGTGGTCGAAATGGCTATGGAGCCAAATTGTGTAACATATTC

AGTACCAAATTTACTGTGGAAACAGCCAGTAGAGAATACAAGAAAATGTTCAAACAG

ACATGGATGGATAATATGGGAAGAGCTGGTGAGATGGAACTCAAGCCCTTCAATGGA

GAAGATTATACATGTATCACCTTTCAGCCTGATTTGTCTAAGTTTAAAATGCAAAGCCT

GGACAAAGATATTGTTGCACTAATGGTCAGAAGAGCATATGATATTGCTGGATCCACC

AAAGATGTCAAAGTCTTTCTTAATGGAAATAAACTGCCAGTAAAAGGATTTCGTAGTT

ATGTGGACATGTATTTGAAGGACAAGTTGGATGAAACTGGTAACTCCTTGAAAGTAAT

ACATGAACAAGTAAACCACAGGTGGGAAGTGTGTTTAACTATGAGTGAAAAAGGCTT

TCAGCAAATTAGCTTTGTCAACAGCATTGCTACATCCAAGGGTGGCAGACATGTTGAT

TATGTAGCTGATCAGATTGTGACTAAACTTGTTGATGTTGTGAAGAAGAAGAACAAG

GGTGGTGTTGCAGTAAAAGCACATCAGGTGAAAAATCACATGTGGATTTTTGTAAATG

CCTTAATTGAAAACCCAACCTTTGACTCTCAGACAAAAGAAAACATGACTTTACAAC

CCAAGAGCTTTGGATCAACATGCCAATTGAGTGAAAAATTTATCAAAGCTGCCATTGG

CTGTGGTATTGTAGAAAGCATACTAAACTGGGTGAAGTTTAAGGCCCAAGTCCAGTTA

AACAAGAAGTGTTCAGCTGTAAAACATAATAGAATCAAGGGAATTCCCAAACTCGAT

GATGCCAATGATGCAGGGGGCCGAAACTCCACTGAGTGTACGCTTATCCTGACTGAG

GGAGATTCAGCCAAAACTTTGGCTGTTTCAGGCCTTGGTGTGGTTGGGAGAGACAAA

TATGGGGTTTTCCCTCTTAGAGGAAAAATACTCAATGTTCGAGAAGCTTCTCATAAGC

AGATCATGGAAAATGCTGAGATTAACAATATCATCAAGATTGTGGGTCTTCAGTACAA

GAAAAACTATGAAGATGAAGATTCATTGAAGACGCTTCGTTATGGGAAGATAATGATT

ATGACAGATCAGGACCAAGATGGTTCCCACATCAAAGGCTTGCTGATTAATTTTATCC

ATCACAACTGGCCCTCTCTTCTGCGACATCGTTTTCTGGAGGAATTTATCACTCCCATT

GTAAAGGTATCTAAAAACAAGCAAGAAATGGCATTTTACAGCCTTCCTGAATTTGAAG

AGTGGAAGAGTTCTACTCCAAATCATAAAAAATGGAAAGTCAAATATTACAAAGGTTT

GGGCACCAGCACATCAAAGGAAGCTAAAGAATACTTTGCAGATATGAAAAGACATCG

TATCCAGTTCAAATATTCTGGTCCTGAAGATGATGCTGCTATCAGCCTGGCCTTTAGCA

AAAAACAGATAGATGATCGAAAGGAATGGTTAACTAATTTCATGGAGGATAGAAGAC

AACGAAAGTTACTTGGGCTTCCTGAGGATTACTTGTATGGACAAACTACCACATATCT

GACATATAATGACTTCATCAACAAGGAACTTATCTTGTTCTCAAATTCTGATAACGAGA

GATCTATCCCTTCTATGGTGGATGGTTTGAAACCAGGTCAGAGAAAGGTTTTGTTTAC

TTGCTTCAAACGGAATGACAAGCGAGAAGTAAAGGTTGCCCAATTAGCTGGATCAGT

GGCTGAAATGTCTTCTTATCATCATGGTGAGATGTCACTAATGATGACCATTATCAATTT

GGCTCAGAATTTTGTGGGTAGCAATAATCTAAACCTCTTGCAGCCCATTGGTCAGTTT

GGTACCAGGCTACATGGTGGCAAGGATTCTGCTAGTCCACGATACATCTTTACAATGC

TCAGCTCTTTGGCTCGATTGTTATTTCCACCAAAAGATGATCACACGTTGAAGTTTTTA

TATGATGACAACCAGCGTGTTGAGCCTGAATGGTACATTCCTATTATTCCCATGGTGCT

GATAAATGGTGCTGAAGGAATCGGTACTGGGTGGTCCTGCAAAATCCCCAACTTTGAT

GTGCGTGAAATTGTAAATAACATCAGGCGTTTGATGGATGGAGAAGAACCTTTGCCA

ATGCTTCCAAGTTACAAGAACTTCAAGGGTACTATTGAAGAACTGGCTCCAAATCAAT

ATGTGATTAGTGGTGAAGTAGCTATTCTTAATTCTACAACCATTGAAATCTCAGAGCTT

CCCGTCAGAACATGGACCCAGACATACAAAGAACAAGTTCTAGAACCCATGTTGAAT

GGCACCGAGAAGACACCTCCTCTCATAACAGACTATAGGGAATACCATACAGATACCA

CTGTGAAATTTGTTGTGAAGATGACTGAAGAAAAACTGGCAGAGGCAGAGAGAGTT

GGACTACACAAAGTCTTCAAACTCCAAACTAGTCTCACATGCAACTCTATGGTGCTTT

TTGACCACGTAGGCTGTTTAAAGAAATATGACACGGTGTTGGATATTCTAAGAGACtTT

TTTGAACTCAGACTTAAATATTATGGATTAAGAAAAGAATGGCTCCTAGGAATGCTTG

GTGCTGAATCTGCTAAACTGAATAATCAGGCTCGCTTTATCTTAGAGAAAATAGATGG

CAAAATAATCATTGAAAATAAGCCTAAGAAAGAATTAATTAAAGTTCTGATTCAGAGG

GGATATGATTCGGATCCTGTGAAGGCCTGGAAAGAAGCCCAGCAAAAGGTTCCAGAT

GAAGAAGAAAATGAAGAGAGTGACAACGAAAAGGAAACTGAAAAGAGTGACTCCG

TAACAGATTCTGGACCAACCTTCAACTATCTTCTTGATATGCCCCTTTGGTATTTAACC

AAGGAAAAGAAAGATGAACTCTGCAGGCTAAGAAATGAAAAAGAACAAGAGCTGG

ACACATTAAAAAGAAAGAGTCCATCAGATTTGTGGAAAGAAGACTTGGCTACATTTAT

TGAAGAATTGGAGGCTGTTGAAGCCAAGGAAAAACAAGATGAACAAGTCGGACTTC

CTGGGAAAGGGGGGAAGGCCAAGGGGAAAAAAACACAAATGGCTGAAGTTTTGCCT

TCTCCGCGTGGTCAAAGAGTCATTCCACGAATAACCATAGAAATGAAAGCAGAGGCA

GAAAAGAAAAATAAAAAGAAAATTAAGAATGAAAATACTGAAGGAAGCCCTCAAGA

AGATGGTGTGGAACTAGAAGGCCTAAAACAAAGATTAGAAAAGAAACAGAAAAGAG

AACCAGGTACAAAGACAAAGAAACAAACTACATTGGCATTTAAGCCAATCAAAAAA

GGAAAGAAGAGAAATCCCTGGtCTGATTCAGAATCAGATAGGAGCAGTGACGAAAGT

AATTTTGATGTCCCTCCACGAGAAACAGAGCCACGGAGAGCAGCAACAAAAACAAA

ATTCACAATGGATTTGGATTCAGATGAAGATTTCTCAGATTTTGATGAAAAAACTGAT

GATGAAGATTTTGTCCCATCAGATGCTAGTCCACCTAAGACCAAAACTTCCCCAAAAC

TTAGTAACAAAGAACTGAAACCACAGAAAAGTGTCGTGTCAGACCTTGAAGCTGAT

GATGTTAAGGGCAGTGTACCACTGTCTTCAAGCCCTCCTGCTACACATTTCCCAGATG

AAACTGAAATTACAAACCCAGTTCCTAAAAAGAATGTGACAGTGAAGAAGACAGCA

GCAAAAAGTCAGTCTTCCACCTCCACTACCGGTGCCAAAAAAAGGGCTGCCCCAAA

AGGAACTAAAAGGGATCCAGCTTTGAATTCTGGTGTCTCTCAAAAGCCTGATCCTGC

CAAAACCAAGAATCGCCGCAAAAGGAAGCCATCCACTTCTGATGATTCTGACTCTAA

TTTTGAGAAAATTGTTTCGAAAGCAGTCACAAGCAAGAAATCCAAGGGGGAGAGTG

ATGACTTCCATATGGACTTTGACTCAGCTGTGGCTCCTCGGGCAAAATCTGTACGGGC

AAAGAAACCTATAAAGTACCTGGAAGAGTCAGATGAAGATGATCTGTTTTAAAATGT

GAGGCGATTATTTTAAGTAATTATCTTACCAAGCCCAAGACTGGTTTTAAAGTTACCTG

AAGCTCTTAACTTCCTCCCCTCTGAATTTAGTTTGGGGAAGGTGTTTTTAGTACAAGA

CATCAAAGTGAAGTAAAGCCCAAGTGTTCTTTAGCTTTTTATAATACTGTaTAAATAGT

GACCATCTCATGGGCATTGTTTTCTTCTCTGCTTTGTCTGTGTTTTGAGTCTGCTTCTTT

TGTCTTTAAAACCTGATTTTTAAGTTCTTCTGAACTGTAGAAATAGCTATCTGATCACT

TCAGCGTAAAGCAGTGTGTTTATTAACCATCCACTAAGCTAAAACTAGAGCAGTTTGA

TTTAAAAGTGTCACTCTTCCTCCTTTTCTACTTTCAGTAGATATGAGATAGAGCATAAT

TATCTGTTTTATCTTAGTTTTATACATAATTTACCATCAGATAGAACTTTATGGTTCTAGT

ACAGATACTCTACTACACTCAGCCTCTTATGTGCCAAGTTTTTCTTTAAGCAATGAGAA

ATTGCTCATGTTCTTCATCTTCTCAAATCATCAGAGGCCGAAGAAAAACACTTTGGCT

GTGTCTATAACTTGACACAGTCAATAGAATGAAGAAAATTAGAGTAGTTATGTGATTAT

TTCAGCTCTTGACCTGTCCCCTCTGGCTGCCTCTGAGTCTGAATCTCCCAAAGAGAGA

AACCAATTTCTAAGAGGACTGGATTGCAGAAGACTCGGGGACAACATTTGATCCAAG

ATCTTAAATGTTATATTGATAACCATGCTCAGCAATGAGCTATTAGATTCATTTTGGGAA

ATCTCCATAATTTCAATTTGTAAACTTTGTTAAGACCTGTCTACATTGTTATATGTGTGT

GACTTGAGTAATGTTATCAACGTTTTTGTAAATATTTACTATGTTTTTCTATTAGCTAAAT

TCCAACAATTTTGTACTTTAATAAAATGTTCTAAACATTGAAAAGGAATTCGATATCAA

GCTTATCGATACCGTCGACTCTAGAGGATCCCCGGGTACCGAGCTCGAATTCACTGGC

CGTCGTTTTACAACGTCGTGACTGGGAAAACCCTGGCGTTACCCAACTTAATCGCCTT

GCAGCACATCCCCCTTTCGCCAGCTGGCGTAATAGCGAAGAGGCCCGCACCGATCGC

CCTTCCCAACAGTTGCGCAGCCTGAATGGCGAATGGCGCCTGATGCGGTATTTTCTCC

TTACGCATCTGTGCGGTATTTCACACCGCATATATCGCTGGGCCATTCTCATGAAGAAT

ATCTTGAATTTATTGTCATATTACTAGTTGGTGTGGAAGTCCATATATCGGTGATCAATA

TAGTGGTTGACATGCTGGCTAGTCAACATTGAGCCTTTTGATCATGCAAATATATTACG

GTATTTTACAATCAAATATCAAACTTAACTATTGACTTTATAACTTATTTAGGTGGTAAC

ATTCTTATAAAAAAGAAAAAAATTACTGCAAAACAGTACTAGCTTTTAACTTGTATCCT

AGGTTATCTATGCTGTCTCACCATAGAGAATATTACCTATTTCAGAATGTATGTCCATGA

TTCGCCGGGTAAATACATATAATACACAAATCTGGCTTAATAAAGTCTATAATATATCTC

ATAAAGAAGTGCTAAATTGGCTAGTGCTATATATTTTTAAGAAAATTTCTTTTGACTAA

GTCCATATCGACTTTGTAAAAGTTCACTTTAGCATACATATATTACACGAGCCAGAAAT

TGTAACTTTTGCCTAAAATCACAAATTGCAAAATTTAATTGCTTGCAAAAGGTCACAT

GCTTATAATCAACTTTTTTAAAAATTTAAAATACTTTTTTATTTTTTATTTTTAAACATAA

ATGAAATAATTTATTTATTGTTTATGATTACCGAAACATAAAACCTGCTCAAGAAAAAG

AAACTGTTTTGTCCTTGGAAAAAAAGCACTACCTAGGAGCGGCCAAAATGCCGAGGC

TTTCATAGCTTAAACTCTTTACAGAAAATAGGCATTATAGATCAGTTCGAGTTTTCTTAT

TCTTCCTTCCGGTTTTATCGTCACAGTTTTACAGTAAATAAGTATCACCTCTTAGAGTT

CGATGATAAGCTGTCAAACATGAGAATTAATTCCACATGTTAAAATAGTGAAGGAGCA

TGTTCGGCACACAGTGGACCGAACGTGGGGTAAGTGCACTAGGGTCCGGTTAAACG

GATCTCGCATTGATGAGGCAACGCTAATTATCAACATATAGATTGTTATCTATCTGCATG

AACACGAAATCTTTACTTGACGACTTGAGGCTGATGGTGTTTATGCAAAGAAACCAC

TGTGTTTAATATGTGTCACTGTTTGATATTACTGTCAGCGTAGAAGATAATAGTAAAAG

CGGTTAATAAGTGTATTTGAGATAAGTGTGATAAAGTTTTTACAGCGAAAAGACGATA

AATACAAGAAAATGATTACGAGGATACGGAGAGAGGTATGTACATGTGTATTTATATAC

TAAGCTGCCGGCGGTTGTTTGCAAGACCGAGAAAAGGCTAGCAAGAATCGGGTCATT

GTAGCGTATGCGCCTGTGAACATTCTCTTCAACAAGTTTGATTCCATTGCGGTGAAAT

GGTAAAAGTCAACCCCCTGCGATGTATATTTTCCTGTACAATCAATCAAAAAGCCAAA

TGATTTAGCATTATCTTTACATCTTGTTATTTTACAGATTTTATGTTTAGATCTTTTATGCT

TGCTTTTCAAAAGGCTTGCAGGCAAGTGCACAAACAATACTTAAATAAATACTACTCA

GTAATAACCTATTTCTTAGCATTTTTGACGAAATTTGCTATTTTGTTAGAGTCTTTTACA

CCATTTGTCTCCACACCTCCGCTTACATCAACACCAATAACGCCATTTAATCTAAGCGC

ATCACCAACATTTTCTGGCGTCAGTCCACCAGCTAACATAAAATGTAAGCTCTCGGGG

CTCTCTTGCCTTCCAACCCAGTCAGAAATCGAGTTCCAATCCAAAAGTTCACCTGTCC

CACCTGCTTCTGAATCAAACAAGGGAATAAACGAATGAGGTTTCTGTGAAGCTGCAC

TGAGTAGTATGTTGCAGTCTTTTGGAAATACGAGTCTTTTAATAACTGGCAAACCGAG

GAACTCTTGGTATTCTTGCCACGACTCATCTCCATGCAGTTGGACGATCGATGATAAG

CTGTCAAACATGAGAATTGGGTAATAACTGATATAATTAAATTGAAGCTCTAATTTGTG

AGTTTAGTATACATGCATTTACTTATAATACAGTTTTTTAGTTTTGCTGGCCGCATCTTC

TCAAATATGCTTCCCAGCCTGCTTTTCTGTAACGTTCACCCTCTACCTTAGCATCCCTT

CCCTTTGCAAATAGTCCTCTTCCAACAATAATAATGTCAGATCCTGTAGAGACCACATC

ATCCACGGTTCTATACTGTTGACCCAATGCGTCTCCCTTGTCATCTAAACCCACACCGG

GTGTCATAATCAACCAATCGTAACCTTCATCTCTTCCACCCATGTCTCTTTGAGCAATA

AAGCCGATAACAAAATCTTTGTCGCTCTTCGCAATGTCAACAGTACCCTTAGTATATTC

TCCAGTAGATAGGGAGCCCTTGCATGACAATTCTGCTAACATCAAAAGGCCTCTAGGT

TCCTTTGTTACTTCTTCTGCCGCCTGCTTCAAACCGCTAACAATACCTGGGCCCACCA

CACCGTGTGCATTCGTAATGTCTGCCCATTCTGCTATTCTGTATACACCCGCAGAGTAC

TGCAATTTGACTGTATTACCAATGTCAGCAAATTTTCTGTCTTCGAAGAGTAAAAAATT

GTACTTGGCGGATAATGCCTTTAGCGGCTTAACTGTGCCCTCCATGGAAAAATCAGTC

AAGATATCCACATGTGTTTTTAGTAAACAAATTTTGGGACCTAATGCTTCAACTAACTC

CAGTAATTCCTTGGTGGTACGAACATCCAATGAAGCACACAAGTTTGTTTGCTTTTCG

TGCATGATATTAAATAGCTTGGCAGCAACAGGACTAGGATGAGTAGCAGCACGTTCCT

TATATGTAGCTTTCGACATGATTTATCTTCGTTTCCTGCATGTTTTTGTTCTGTGCAGTT

GGGTTAAGAATACTGGGCAATTTCATGTTTCTTCAACACTACATATGCGTATATATACCA

ATCTAAGTCTGTGCTCCTTCCTTCGTTCTTCCTTCTGTTCGGAGATTACCGAATCAAAA

AAATTTCAAAGAAACCGAAATCAAAAAAAAGAATAAAAAAAAAATGATGAATTGAAT

TGAAAAGCTAATTCTTGAAGACGAAAGGGCCTCGTGATACGCCTATTTTTATAGGTTA

ATGTCATGATAATAATGGTTTCTTAGACGTCAGGTGGCACTTTTCGGGGAAATGTGCG

CGGAACCCCTATTTGTTTATTTTTCTAAATACATTCAAATATGTATCCGCTCATGAGACA

ATAACCCTGATAAATGCTTCAATAATATTGAAAAAGGAAGAGTATGAGTATTCAACATT

TCCGTGTCGCCCTTATTCCCTTTTTTGCGGCATTTTGCCTTCCTGTTTTTGCTCACCCA

GAAACGCTGGTGAAAGTAAAAGATGCTGAAGATCAGTTGGGTGCACGAGTGGGTTA

CATCGAACTGGATCTCAACAGCGGTAAGATCCTTGAGAGTTTTCGCCCCGAAGAACG

TTTTCCAATGATGAGCACTTTTAAAGTTCTGCTATGTGGCGCGGTATTATCCCGTATTG

ACGCCGGGCAAGAGCAACTCGGTCGCCGCATACACTATTCTCAGAATGACTTGGTTG

AGTACTCACCAGTCACAGAAAAGCATCTTACGGATGGCATGACAGTAAGAGAATTAT

GCAGTGCTGCCATAACCATGAGTGATAACACTGCGGCCAACTTACTTCTGACAACGAT

CGGAGGACCGAAGGAGCTAACCGCTTTTTTGCACAACATGGGGGATCATGTAACTCG

CCTTGATCGTTGGGAACCGGAGCTGAATGAAGCCATACCAAACGACGAGCGTGACAC

CACGATGCCTGTAGCAATGGCAACAACGTTGCGCAAACTATTAACTGGCGAACTACTT

ACTCTAGCTTCCCGGCAACAATTAATAGACTGGATGGAGGCGGATAAAGTTGCAGGA

CCACTTCTGCGCTCGGCCCTTCCGGCTGGCTGGTTTATTGCTGATAAATCTGGAGCCG

GTGAGCGTGGGTCTCGCGGTATCATTGCAGCACTGGGGCCAGATGGTAAGCCCTCCC

GTATCGTAGTTATCTACACGACGGGGAGTCAGGCAACTATGGATGAACGAAATAGACA

GATCGCTGAGATAGGTGCCTCACTGATTAAGCATTGGTAACTGTCAGACCAAGTTTAC

TCATATATACTTTAGATTGATTTAAAACTTCATTTTTAATTTAAAAGGATCTAGGTGAAG

ATCCTTTTTGATAATCTCATGACCAAAATCCCTTAACGTGAGTTTTCGTTCCACTGAGC

GTCAGACCCCGTAGAAAAGATCAAAGGATCTTCTTGAGATCCTTTTTTTCTGCGCGTA

ATCTGCTGCTTGCAAACAAAAAAACCACCGCTACCAGCGGTGGTTTGTTTGCCGGAT

CAAGAGCTACCAACTCTTTTTCCGAAGGTAACTGGCTTCAGCAGAGCGCAGATACCA

AATACTGTCCTTCTAGTGTAGCCGTAGTTAGGCCACCACTTCAAGAACTCTGTAGCAC

CGCCTACATACCTCGCTCTGCTAATCCTGTTACCAGTGGCTGCTGCCAGTGGCGATAA

GTCGTGTCTTACCGGGTTGGACTCAAGACGATAGTTACCGGATAAGGCGCAGCGGTC

GGGCTGAACGGGGGGTTCGTGCACACAGCCCAGCTTGGAGCGAACGACCTACACCG

AACTGAGATACCTACAGCGTGAGCTATGAGAAAGCGCCACGCTTCCCGAAGGGAGA

AAGGCGGACAGGTATCCGGTAAGCGGCAGGGTCGGAACAGGAGAGCGCACGAGGG

AGCTTCCAGGGGGAAACGCCTGGTATCTTTATAGTCCTGTCGGGTTTCGCCACCTCTG

ACTTGAGCGTCGATTTTTGTGATGCTCGTCAGGGGGGCGGAGCCTATGGAAAAACGC

CAGCAACGCGGCCTTTTTACGGTTCCTGGCCTTTTGCTGGCCTTTTGCTCACATGTTCT

TTCCTGCGTTATCCCCTGATTCTGTGGATAACCGTATTACCGCCTTTGAGTGAGCTGAT

ACCGCTCGCCGCAGCCGAACGACCGAGCGCAGCGAGTCAGTGAGCGAGGAAGCGG

AAGAGCGCCCAATACGCAAACCGCCTCTCCCCGCGCGTTGGCCGATTCATTAATGCA

GCTGGCACGACAGGTTTCCCGACTGGAAAGCGGGCAGTGAGCGCAACGCAATTAAT

GTGAGTTAGCTCACTCATTAGGCACCCCAGGCTTTACACTTTATGCTTCCGGCTCGTAT

GTTGTGTGGAATTGTGAGCGGATAACAATTTCACACAGGAAACAGCTATGACCATGAT

TACGCCAAGCTTGGCGCCCTGAAGACAAATTTCGAAACCGAGTGGAACCTGCAAACT

CTAGCCGCCGACGACGCATTTTGATATATAGGAGTTTAATACTATAGCCATAAAATCTA

AACAGAATGGAAACGGACATACACATAATATACGCTCATATATATTTATACATAACTTCA

ATGTCTTGAACACGTAAATTTTAGTGTGAGAAACCTTTTTCACTCCGGGTAATACCTG

CTGTAGTCTTCAAAAAAAAAAAAAAAAAGAAAAAAAACCAGCCATGGAAAGCTCT

TTATTTTTTTACTTTACGGCTTTTTTCCCTTTTCTTATATGATCGATGCACGTAAAGAAC

AACTGTATTTTTTTGTTTCAACACTAACACGAGCGCAATATTCTTTTTTGTTTTCTCTGT

TACTCTAATTACCTGAGTCCTATTCTTATAGTATTAAAACAGCAAATAAAAAAAATCTA

AAGGGAGGGCAGAGCTCGAAACTTGAAACGCGTCC

Appendix D List of Abbreviations Used

- X###X': Format for amino acid mutations. First letter is original amino acid, number is amino acid location, final letter is resulting amino acid (e.g., R450Q is an arginine mutating to a glutamine at the 450th amino acid position)
- A: Alanine (Nonpolar)
- V: Valine (Nonpolar)
- I: Isoleucine (Nonpolar)
- L: Leucine (Nonpolar)
- M: Methionine (Nonpolar)
- F: Phenylalanine (Nonpolar)
- W: Tryptophan (Nonpolar)
- G: Glycine (Nonpolar)
- P: Proline (Nonpolar)
- C: Cysteine (Nonpolar)
- S: Serine (Polar Uncharged)
- T: Threonine (Polar Uncharged)
- N: Asparagine (Polar Uncharged)
- Q: Glutamine (Polar Uncharged)
- R: Arginine (Polar Positive)
- H: Histidine (Polar Positive)
- K: Lysine (Polar Positive)
- D: Aspartic Acid (Polar Negative)
- Glutamic Acid (Polar Negative)

- WHO: World Health Organization
- NCI: National Cancer Institute
- ACS: American Cancer Society
- PCR: Polymerase Chain Reaction
- WT: Wild-Type (unmutated Human Topoisomerase II-alpha)
- pMJ1: Obtained plasmid from Dr. John Nitiss containing Human Topoisomerase II-alpha gene
- ATGC: DNA Nucleotides Adenine, Thymine, Guanine, Cytosine
- URA- Plates: Plates fostering cell growth lacking uracil
- Ymtt: Temperature sensitive yeast strain
- BLAST: Basic Local Alignment Search Tool
- CFU: Colony Forming Unit
- TOPRIM: Topoisomerase-Primase
- hTOP2A: Gene encoding Human Topoisomerase IIα